Controlling the power of the ground by integration

D2.4

Quantified differences in optimal TABS, HP and GSHX sizing for MPC and RBC

Author(s): **UGent & KU Leuven**

Date: **September 25th, 2020 (M49)**

Version: 1.0

Dissemination level: Public

Funded by the European Commission under the Horizon 2020 Programme: project number 723649 (proposal name "MPC-;GT")

hybridGEOTABS www.hybridgeotabs.eu

Lead beneficiary: BOY (Boydens Engineering, Belgium)

Deliverable lead: UGent (Ghent University, Belgium)

Author(s): KU Leuven (Katholieke Universiteit Leuven, Belgium)

Filip Jorissen (filip.jorissen@kuleuven.be)

Lieve Helsen (lieve.helsen@kuleuven.be)

UGent (Ghent University, Belgium)

Mohsen Sharifi (mohsen.sharifi@ugent.be)

Eline Himpe (eline.himpe@ugent.be)

Jelle Laverge (jelle.laverge@ugent.be)

Reviewer(s): BOY (Boydens Engineering, Belgium)

Wim Boydens

Dissemination level: Public

DOI : https://doi.org/10.5281/zenodo.4892351

Summary

The hybridGEOTABS system consist of a primary and secondary heating and cooling system. The primary and preferential system is the GEOTABS system, in which the geothermal heat pump (HP), the geothermal borefield or ground-source heat exchanger (GSHX) and the thermally activated building system (TABS) are key components. The secondary system (SS) components are a fast-reacting emission system (e.g. variable air volume systems (VAV), fan coil units (FCU), radiators, convectors etc.) and a heat/cold production system, for which many renewable and non-renewable options exist as well (e.g. gas boiler, air-source heat pump, chiller, solar boiler, biomass boiler, district heating etc.) (see D6.1). In this study a non-renewable baseline secondary system is selected (conform the baseline definitions in D4.5), consisting of fan coil units coupled to a gas condensing boiler for heating and a chiller for cooling. Those are the key components of the secondary system in this report. The secondary heating and/or cooling system comes in at times that using the GEOTABS system is not preferential or feasible, aiming at climatising the building at every moment in an environmentally friendly and cost-effective way. To achieve this aim, an adequate controller is required that optimises the decision between primary and secondary system, and between heating and cooling of the building zones. Therefore, the hybridGEOTABS solution includes a model predictive controller (MPC) that is able to make this choice in a much smarter way than the current practice rule-based controllers (RBC). A well-designed MPC will use whatever system components and powers available more efficiently in order to minimise the cost and/or environmental impact while reaching thermal comfort. Vice versa, one may understand that if we know the behaviour of the smart controller already during the design of the HVAC-system, we may make a more optimal sizing of the key components, which will again improve the cost- and environmental efficiency of the building HVAC. This is what we call a *control-integrated design*.

In the design stage, and especially in the early design stages, the decision on the sizing of primary and secondary systems is not an easy choice, but has a big impact on the cost-effectiveness and thus feasibility of the HVAC-concept, and on its energy performance. The development of a design strategy for optimal sizing of hybridGEOTABS system components in feasibility and pre-design stage, is the main objective of this work package (WP2). The approach to come to this design methodology includes the building energy simulations of a large amount of building cases from the EU building stock (T2.2), the use of a computationally fast load splitting algorithm (T2.1) and post-processing of its outcomes to come to a sizing of the key hybridGEOTABS system components (HP (&TABS), GSHX, SS) for a variety of cases appearing in the EU building stock (T2.4-2.5). To arrive to this computationally fast strategy, the use of simplifications is inevitable. One such simplification is the level of detail in which the HVAC-systems and controls, and their interaction with the building, are dealt with in the T2.1 baseload splitting algorithm. Therefore, in this task (T2.3), that aspect is studied more in detail.

In the first part of task 2.3, reported in D2.3, a nested optimisation algorithm was developed that integrates the HVAC design and control. In summary, the algorithm includes the HVAC design (= the sizes for the key components) as optimisation variable, and for each design an optimal model predictive controller is automatically generated. The optimal design is the design for which the net present cost is largest (taking into account constraints such as thermal comfort and borefield balance) and is obtained using a non-linear program (NLP) solver. The controller itself is a simplified version of the white-box MPC's developed in T3.1, by using optimized heating and cooling curves. This simplification of the controller for the design exercise is needed to make the work computationally feasible: the actual building controllers in T3.1 are made to optimize a very detailed HVAC-system model of a specific building over a period of a few days, while a control-integrated optimised design requires an optimisation over the building lifetime of 25 years ànd calculation of a multitude of design options (combinations of sizes of the key components) for multiple cases, which would lead to an explosion of the computation time.

In the second part of task 2.3, documented in the underlying D2.4, the nested optimisation algorithm with MPC (the 'MPC-approach') is applied to selected cases and compared to a design optimisation with current practice

RBC (the 'RBC-approach'). The optimal design with the current practice RBC is obtained by simulating a current practice RBC (a typical heating curve) for a set of HVAC designs, and selecting the design that minimizes the net present cost under the given constraints. This exercise allows to obtain an indication of the differences in optimal sizing of the HVAC key components in a hybridGEOTABS system as a result of the choice of controller.

The investigated cases are a selection of 9 variations of an office building from the building stock cases (T2.2). The variations represent different building physical properties (e.g. insulation level, occupancy profiles, shading systems) and 3 different climates representing the main EU climates[1].

This report documents the control-integrated design methodologies with MPC and RBC (section 2) and the verification of key aspects of this methodology (section 3). Next, the case-studies are introduced (section 4). Finally, the MPC- and RBC-approaches are applied to the case-studies and the differences in key performance indicators are analysed (section 5). The key performance indicators are the financial cost, environmental and energy performance and the sizing of the key components.

It is concluded that by using the MPC-approach as opposed to a design optimisation with current practice RBC, the optimisation leads to a reduction in the financial cost of the HVAC-system, as indicated by the net present cost, and a reduction of the environmental and energy impact as indicated by the CO_2-emissions and primary energy use. The values are case-dependent, and for the 5 cases in this study the reductions go from a few percentages up to significant reductions of 20% for the net present value, 28% for the CO2-emissions and 26 % for the primary energy use.

Behind these numbers, throughout the cases a consistent tendency is observed: the control-integrated optimisation (the MPC-approach) leads to a decrease in the size and investment cost for the secondary HVAC-system together with a reduced energy generation and operating costs. This reduction of the secondary system goes together with an increase in the amount of energy provided by the GEOTABS system to the building (which aligns with a similar or increased size of the geothermal borefield), combined with a significant reduction (between 13% and 60%) in the heat pump size due to the more efficient MPC control. In conclusion, the hybridGEOTABS system MPC-integrated design leads to an increase in the use of GEOTABS (to more than 80% of the overall heating and cooling energy use of the building in the cases studied) which is beneficial from both financial and environmental point of view.

Finally, the installed powers of primary and secondary systems together can also be compared to the design powers for heating and cooling as calculated by standardised steady-state heat loss calculations, that are used in traditional design practice. They show a remarkable potential for downsizing the hybridGEOTABS components. It is observed that by using the control-integrated design the overall heating and cooling powers for hybridGEOTABS are reduced by between 16% and 62% for both heating and cooling when the RBC-approach is used, and by 52% to 77% when the MPC-approach is used. This illustrates the need ànd the value of an integrated sizing methodology for hybridGEOTABS systems that takes into account the properties of TABS, the interactions between primary and secondary systems and the control as system-integrator.

The findings from this study on a limited amount of case-study buildings are used in the subsequent tasks of this work package (T2.4-T2.5) in an additional validation of the more simplified and computationally faster design strategy that is based on the application of the baseload algorithm (T2.1), that also integrates control-aspects in the design albeit in a more simplified way, and the building stock simulation results (T2.2).

---

[1] To align the processes in WP2 tasks, especially to allow comparability of the results with the results from the T2.1 and T2.4 work, it was decided to use these cases from the building stock in T2.2, and not the emulator models from the project case-study and demonstration buildings.

Table of Contents

Nomenclature

Acronyms

AHU	Air Handling Unit
BTES	Borehole Thermal Energy Storage
CCA	Concrete Core Activation
COP	Coefficient of Performance
CO_2	Carbon Dioxide
FCU	Fan Coil Unit
GEOTABS	system combining TABS and geothermal energy using a heat pump
GSHP	Ground Source Heat Pump
GSHX	Ground Source Heat Exchanger
HP	Heat Pump
HVAC	Heating, Ventilation and Air Conditioning
KPI	Key Performance Indicator
MPC	Model Predictive Control
NPC	Net Present Cost
NPV	Net Present Value
PS	Primary system (= GEOTABS)
PV	Photovoltaic
RBC	Rule-based Control
RES	Renewable energy sources
R^2ES	Renewable and residual energy sources
SS	Secondary system
TABS	Thermally Active Building System
TADO	Toolchain for Automated Design and Optimisation
VAV	Variable Air Volume system

1. Introduction

The hybridGEOTABS system consists of a primary and secondary heating and cooling system. The primary and preferential system is the GEOTABS system, in which the geothermal heat pump (HP), the geothermal borefield or ground-source heat exchanger (GSHX) and the thermally activated building system (TABS) are key components. The secondary system components are a fast-reacting emission system (e.g. variable air volume systems (VAV), fan coil units (FCU), radiators, convectors etc.) and a heat/cold production system, for which many renewable and non-renewable options exist as well (e.g. gas boiler, air-source heat pump, chiller, solar boiler, biomass boiler, district heating etc.) (see D6.1 [1]). In this study a non-renewable baseline secondary system is selected, such that it is a worst-case (because alternative secondary systems will mainly improve the environmental performance) but realistic scenario for hybridGEOTABS. Conform the baseline definitions set out in the project, it consists of fan coil units coupled to a gas condensing boiler for heating and a chiller for cooling, see Figure 1 (D4.5 [2]). Those are the key components of the secondary system in this exercise. This combination of components is chosen as it is a feasible solution throughout all the climates and building typologies studied in the project. The secondary heating and/or cooling system comes in at times that using the GEOTABS system is not preferential or feasible, aiming at climatising the building at every moment in an environmentally friendly and cost-effective way. To achieve this aim, an adequate controller is required that optimises the decision between primary and secondary system, and between heating and cooling of the building zones. Therefore, the hybridGEOTABS solution includes a model predictive controller (MPC) that is able to make this choice in a much smarter way than the current practice rule-based controllers (RBC). A well-designed MPC will use whatever system components and powers available more efficiently in order to minimise the cost and/or environmental impact while reaching thermal comfort. Vice versa, one may understand that if we know the behaviour of the smart controller already during the design of the HVAC-system, we may make a more optimal sizing of the key components, which will again improve the cost- and environmental efficiency of the building HVAC. This is what we call a *control-integrated design*.

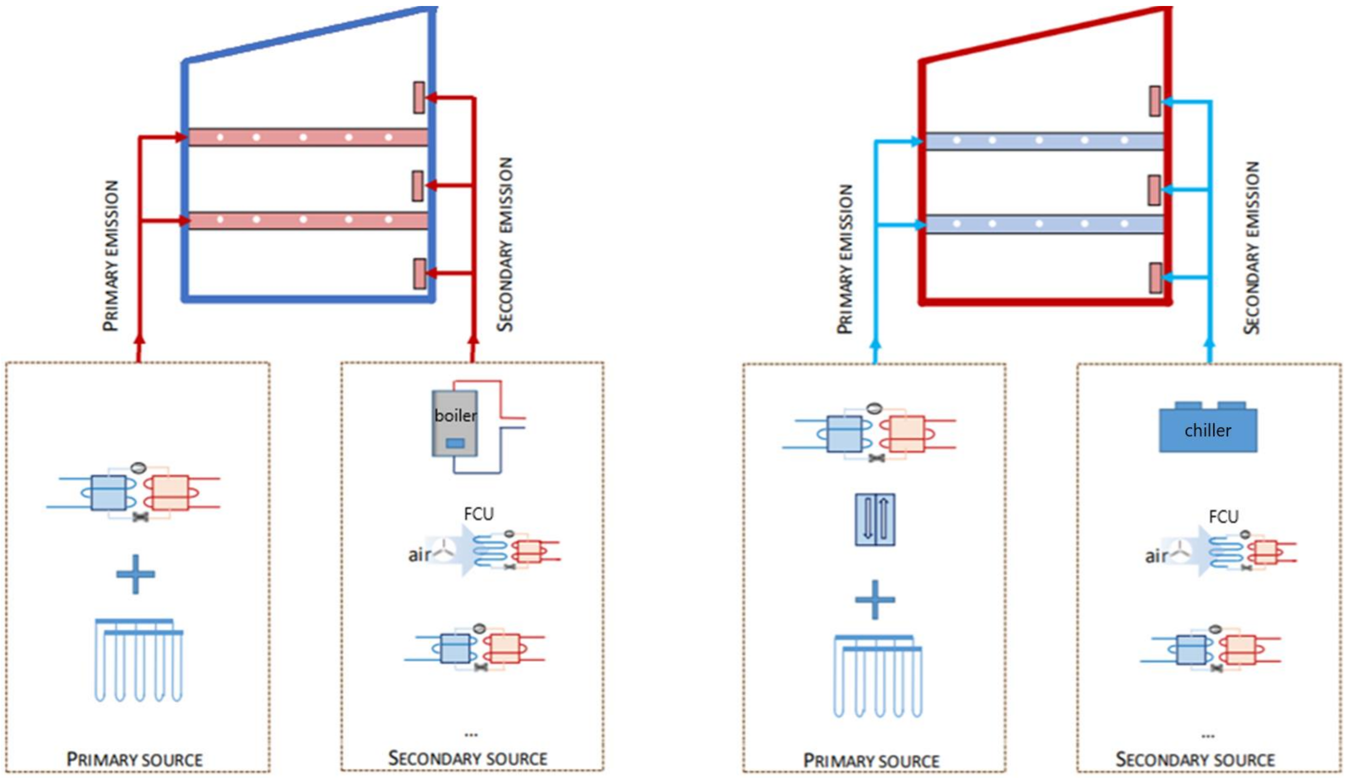

Figure 1: schematic of hybridGEOTABS components in heating (left) and cooling (right)

In the first part of task 2.3, a nested optimisation algorithm was developed that integrates the HVAC design and control (see D2.3 [3]). In summary, the algorithm includes the HVAC design (= the sizes for the key components) as optimisation variable, and for each design an optimal model predictive controller is automatically generated. The optimal design is the design for which the net present cost is largest (taking into account constraints) and is obtained using an NLP solver.

In this exercise, the nested optimisation algorithm with MPC (the 'MPC-approach') is applied to selected cases and compared to a design optimisation with current practice RBC (the 'RBC-approach'). The optimal design with the current practice RBC is obtained by simulating a current practice RBC (a typical heating curve) for a set of HVAC designs, and selecting the design that minimizes the overall cost under the given constraints. This exercise allows to obtain an indication of the differences in optimal sizing of the HVAC key components in a hybridGEOTABS system as a result of the choice of controller, that is RBC and MPC. The control-integrated design methodologies with MPC and RBC are explained in section 2. In section 3 the key aspects of this methodology are verified.

The investigated cases are a selection of 9 variations of an office building from the building stock cases. The variations represent different building physical properties (e.g. insulation level, occupancy profiles, shading systems) and 3 different climates representing the main EU climates. The cases are introduced in section 4.

Finally, in section 5, the MPC- and RBC-approaches are applied to the case-studies and the differences in key performance indicators are studied: financial cost as indicated by the net present cost, environmental performance as indicated by CO_2-emissions, energy performance as indicated by primary energy and load splitting and the sizing (power) of the key components.

2. Methodology: modelling

This section describes the overall optimal design methodology, which consists of two independent approaches. The first approach is called the RBC approach, which relies on running (many) computer simulations of building HVAC-designs with an RBC using JModelica. The second approach is called the MPC approach, which uses the gradient-based optimization algorithm of TADO (Toolchain for Automated Design and Optimization) with an MPC. Both approaches minimize the same *objective function*, the total cost of the system design, which includes both the investment and the operational costs over a period of 25 years.

Both approaches rely on a computer model of the building that is to be designed. Both design approaches aim to find the best values of a set of design variables (optimization variables), such as the bore field size, see Figure 2. The main difference between the two approaches is that the optimization-based MPC approach requires gradient information. More specifically, the partial derivatives of the objective function (and constraints) with respect to all optimization variables must be known. These values express how the objective function changes (increases or decreases) for a change in optimization variable. This information is used to modify the optimization variable values in such a way that the objective function decreases, until it can decrease no further, when we say that the optimization has *converged*. The fact that we require this gradient information puts important limitations on the type of mathematical model that is used. Consequently, the RBC approach allows using more detailed models. This however comes at the cost of computation time, especially when a large number of design variables is chosen, since the MPC approach can compute the influence of all optimization variables simultaneously. Furthermore, the MPC approach is better equipped to deal with constraints, most notably the borefield ground thermal balance, since the constraint gradients allow to compute how optimization variables should be chosen in order for the model constraints to be satisfied, and adjust them accordingly. For the RBC approach this is not possible and therefore we can only verify (i.e. not enforce) whether the ground thermal balance is maintained, and reject a design option when this is not the case. As indicated in Figure 2, the optimal results from the MPC approach, which uses a simplified model, are input into the more detailed simulation model. This way an objective comparison can be made between two approaches such that simplifications in the optimization model do not lead to an unfair advantage compared to the other model. Since the model mismatch may introduce a constraint violation, the constraints are also verified.

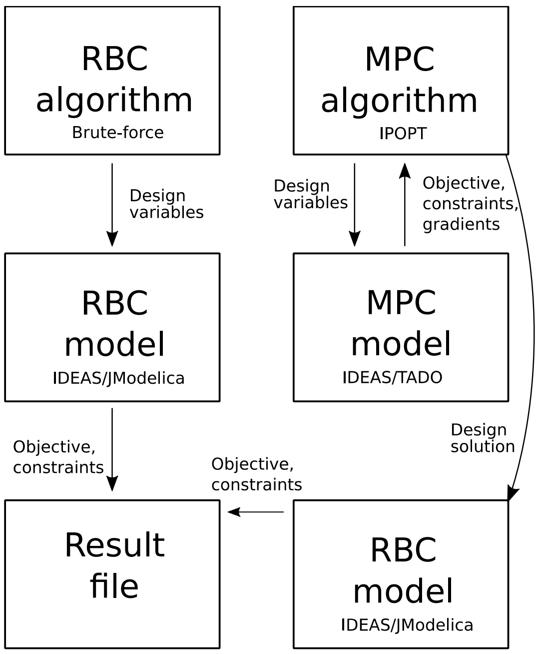

Figure 2: Algorithm and model overview

To summarize: the RBC approach runs many detailed computer simulations, for which the best solution that satisfies the constraints is identified as 'optimal', while the MPC approach changes the optimization variables in a direction that leads to the minimum cost while also satisfying the constraints.

2.1. Modelica models

Figure 2 indicates that two simulation models exist, one for the RBC approach and one for the MPC approach. The RBC model is re-used (with minimal changes) to compare the RBC results with the MPC results as indicated in the bottom right of Figure 3.

Building envelope

Both models use the same building envelope model, which includes the room energy balance, solar/window heat gains, shading and internal heat gains from occupants and appliances. The only difference is that thermal convection is linearized (= slightly simplified) for the MPC model. This way we ensure that both models have a very similar heat demand. The use of high-fidelity models for optimization is an important advantage of our MPC approach since usually such models are highly simplified. Such simplifications and the corresponding model mismatch can easily introduce ground thermal imbalances over the period of the building lifetime, which could lead to ground depletion.

Building HVAC

The building HVAC model consists of 1) the ventilation model, 2) the primary heating system, 3) the secondary heating system, 4) the borefield model. Parts 1 to 3 are illustrated in Figure 3.

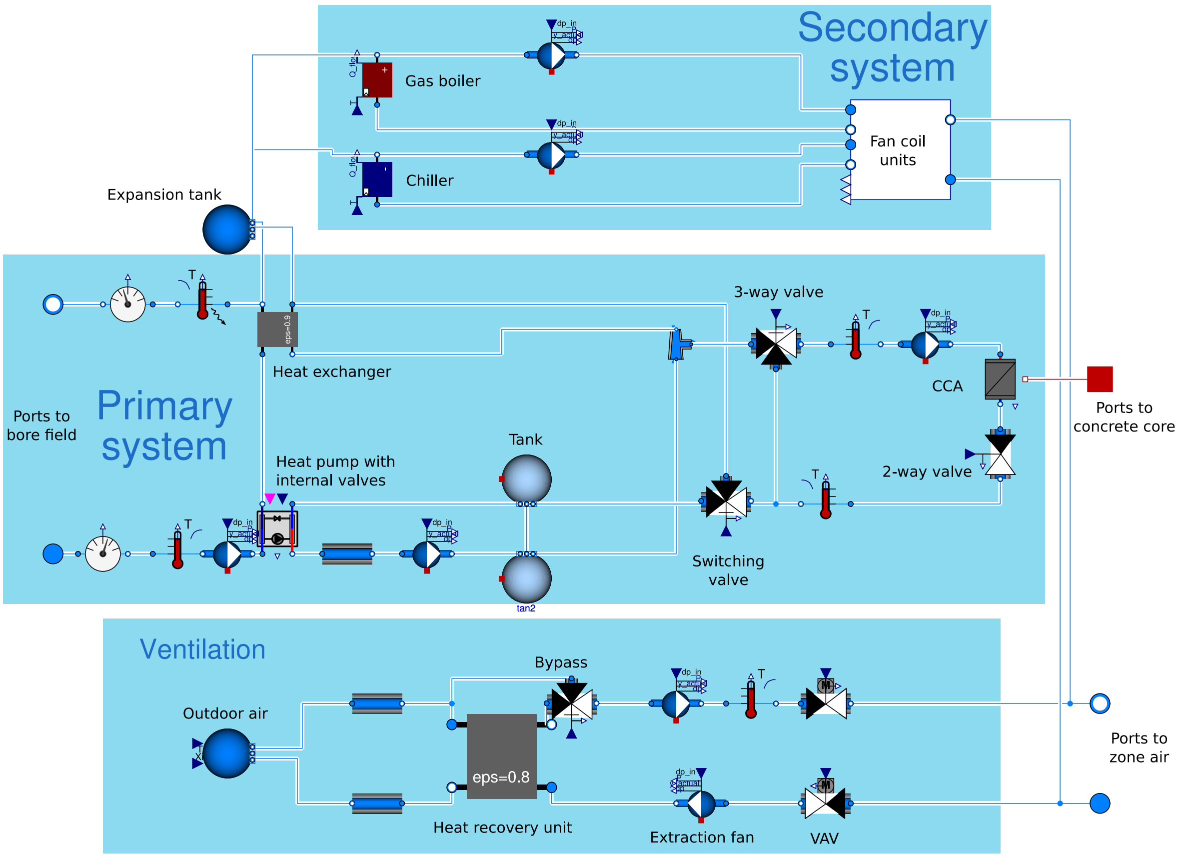

Figure 3: Overview of detailed HVAC model

Ventilation model

Both models use the same ventilation model, which is indicated in the bottom of Figure 3. The ventilation model uses a single supply and return fan with a fixed head of 300 Pa to supply fresh air to all zones. A balanced flow rate of 1.2 ACH is tracked by the VAVs during office hours and 0.12 ACH outside office hours. Heat is recovered with a constant effectiveness of 80 %. A bypass allows to bypass a fraction of the supply air past the heat recovery unit.

Primary heating system

For the **RBC (simulation)** model, the primary heating system consists of an on/off water-water heat pump, circulation pumps, a heat exchanger, three-way valves for switching between cooling and heating mode (included in the heat pump model, not shown in Figure 3), a thermal storage tank to buffer on/off cycles, a three-way valve that controls the supply water temperature, one embedded pipe per zone to model the Concrete Core Activation (CCA) and one two-way valve per floor to control the CCA flow rate of that floor. A switching valve switches between the heat pump and heat exchanger. Note that the schematic does not make a distinction between individual components and vectors of components. More specifically, the VAVs, fan coil units, CCA and 2-way valves are vectors that are connected in parallel to the components that are indicated on the schematic.

The **heat pump model** implements a thermodynamic cycle and as such is able to accurately compute the heat pump thermal powers and electrical power use. The model has been implemented by Cimmino and Wetter [4] and validated by Jorissen [5] for a Viessmann Vitocal 300G BW 301.A45 heat pump. This heat pump model is extended using three-way valves (not visible in Figure 3) to allow both heating and cooling operation. A bypass valve, circulation pump and PI controller are included to ensure that the evaporator inlet temperature does not exceed 15 degrees Celsius, to avoid exceeding the upper bound of the heat pump evaporator inlet temperature.

We assume that the CCA are used for the entire floor surface area, with a pipe spacing of 15 cm. The two-way valves are sized such that a nominal flow rate of 10 $l/h/m^2$ is obtained.

We assume a constant heat exchanger effectiveness of 90 %.

For the **MPC** model, the primary system complexity is reduced considerably. We directly prescribe the concrete core temperature and compute the heat flow rate that is required to achieve this temperature. The resulting heat flow rate is translated into an electrical power consumption using a fixed COP of 6.75 for heating and 7.5 for cooling. The total heat flow rate is limited to the rated heat pump power, multiplied by 1.2 in heating mode and 1.5 in cooling mode, based on manufacturer data. These multiplication factors consider that the heat pump can deliver higher than rated thermal powers at the low temperature differences of the hybridGEOTABS concept.

Secondary heating system

Both models use the same secondary system model, which consists of an ideal heater that supplies warm water at a temperature of 45 °C, a chiller that supplies chilled water at a temperature of 7 °C and a set of 4-pipe Jaga Briza 22 Fan Coil Units. The FCU model contains two internal two-way valves that control the mass flow rate through a heating coil and a cooling coil. A gas boiler efficiency of 98 % and chiller COP of 3 are assumed.

Borefield model

The RBC model uses the borefield model of [3]. It computes the thermal response of the borefield using a temporal and spatial superposition method. A geometry of 2 x 3 boreholes is assumed, which are configured in a square grid with edges of 6 m. We further assume that the soil consists of sandstone, that the borehole diameter is 15 cm and that the borehole has a specific thermal resistence of 0.1 mK/W. The borefield height is the optimized variable.

This detailed model is not supported by the optimization framework. Therefore, a simplified geothermal borefield RC-model was developed within this project that is sufficiently accurate to compute the ground thermal balance over a period of 25 years, for different borefield heights, which is the optimised variable.

The undisturbed ground temperature is an important parameter of the borefield model. It is updated based on the geographic location of the building. An overview of the considered locations and matching temperatures is given in Table 1.

Table 1: Considered locations and yearly averaged temperatures

Location	*Brussels*	*Madrid*	*Warsaw*
Yearly averaged temperature	10.2 ˚C	13.7 ˚C	7.7 ˚C

Building control

The RBC approach implements an RBC for controlling the valves, heat pump and pumps in order to obtain realistic results. Since the same HVAC system and RBC, including the RBC parameters, will be used for many different building envelopes, climates and internal heat gain profiles, which may result in both heating dominated or cooling dominated buildings, design of this controller is hard. In practice a GEOTABS system requires manual tuning of the controller set points (parameters) to achieve reasonable results, which is not practically possible since many hundreds of simulations will be performed. Therefore, a satisfactory default control strategy had to be designed for the RBC approach, which is now described.

We distinguish three building control models:

1. The control model of the RBC model. (For the model in the middle left in Figure 2.)
2. The control model of the MPC model. (For the model in the middle right in Figure 2.)
3. A slightly modified version of the RBC model for validating the MPC model. (For the model in the bottom right in Figure 2.)

We first describe the control models of 1) and 2) and then describe changes of 3) relative to 1).

Building modes

Buildings that use CCA typically use a 'mode' to determine whether the building requires heating, cooling, or none of both. Typical building controllers use average outdoor temperatures to determine this mode. However, such threshold would be hard to generalize due to the range of climates and internal heat gain profiles that are considered. Therefore, we use a different approach.

For both models the building mode is computed using the annual heat loss profile of the building envelope $\dot{Q}(t)$, which is computed beforehand. After a 1-year simulation, the time-averaged maximum cooling power $\dot{Q}_{min}$ and heating power $\dot{Q}_{max}$ of that year are stored. When $\dot{Q}(t)$ exceeds 20 % of $\dot{Q}_{max}$ then the building is said to be in heating mode, otherwise if $\dot{Q}(t)$ exceeds 20 % of $\dot{Q}_{min}$ then the building is in cooling mode, otherwise it is in neutral mode. The neutral mode is implemented to avoid that the building would switch between cooling and heating mode multiple times within the same day, which would lead to cooling and heating peaks, as well as heat exchange within the concrete without reaching the building zone air when the CCA switches between cooling and heating mode.

Ventilation control

All models have a schedule that determines the ventilation mass flow rate. The ventilation system bypass is always closed for the MPC model, such that maximum heat or cold recovery is used. For the RBC model, during heating and neutral mode, the bypass is closed, while during cooling mode a PI controller tracks a supply air temperature of 16 ˚C to use free cooling if it is available.

Secondary system control

For both models, the chiller has a fixed supply water temperature of 7 ˚C and the boiler has a fixed supply water temperature of 45˚C. Both models use the same internal FCU controller. This controller opens a two-way valve when the FCU air inlet temperature threshold of 24 ˚C for cooling and 22˚C for heating is exceeded. The valve opening increases linearly with the air temperature until it is fully opened at a temperature of 25 ˚C for cooling and 21 ˚C for heating. Furthermore, there is a fan control signal that determines the air mass flow rate through the two FCU coils. The model assumes that the air mass flow rate increases linearly with the maximum of the two valve control signals. The FCU heat flow rates are computed from the air and water mass flow rates using a heat exchanger model that is calibrated to the Jaga Briza FCU.

Primary system control of the RBC model

The primary system control of the RBC model further specifies the modes, which can be:

1. Active heating using the geothermal borefield and the heat pump.
2. Passive heating using the geothermal borefield and the heat exchanger.
3. Neutral
4. Passive cooling using the geothermal borefield and the heat exchanger.
5. Active cooling using the geothermal borefield and the heat pump.

Passive cooling is enabled only if the borefield return water temperature is low enough to reach the CCA supply water temperature set point in cooling mode. Vice-versa, the passive heating mode is enabled if the borefield return water temperature is high enough to reach the CCA supply water temperature set point in heating mode.

Based on these modes, either the heat pump or the heat exchanger is connected to the borefield using the switchover valve. The heat pump is enabled when the following conditions are satisfied:

1. The mode is 1 or 5
2. The borefield inlet temperature limits are not exceeded. When they are exceeded, the heat pump is disabled until the end of the day.
3. The storage tank temperature is smaller than the CCA supply water temperature set point in heating mode, or larger in cooling mode.

The heat pump is then enabled until the storage tank temperature exceeds the required set point by ±3 K, for heating and cooling.

For cooling mode, the CCA supply water temperature set point is 19 ˚C. The set point is fixed to a low value, yet not that low that condensation is likely to occur. For heating mode, the CCA supply water temperature set point is the CCA heating set point temperature (24 ˚C) plus $2^{\circ}C\ sca$ where sca is the heat pump scaling factor and 2˚C is the temperature difference that was used to determine the rated heat pump size. The supply water temperature is increased depending on the heat pump size such that the emission system is able to distribute the larger heat pump thermal powers regardless of the nominal emission system mass flow rates. This supply water set point is tracked using the three-way valve and a PI controller. In neutral mode the three-way valve is closed such that water recirculates and redistributes heat and cold between the different building floors.

Each floor has its own two-way valve that controls the flow rate through all parallel CCA sections of the floor. The return water temperature set point is 24 °C during heating mode and 22 °C during cooling mode. These set points are tracked using PI controllers. The valves are fully opened during neutral mode, in order for excess heat or cold to be redistributed across the different floors.

Primary system control of the MPC model

The primary HVAC system of the MPC model has an abstract implementation that does not clearly separate HVAC and controls. Therefore, the approach was partly described when discussing the HVAC system but we extend it here.

The MPC model optimizes the temperature of the concrete core of the CCA indirectly, using a heating curve. The model computes the heat flow rate that is required for reaching this set point in each CCA section. When the total heat flow rate exceeds the available system power, the thermal power of each CCA section is limited such that the total thermal power equals the heat pump thermal power. The resulting thermal powers are injected in the CCA.

Note that (for sufficiently low flow rates) the return water temperature of CCA equals the concrete core temperature of the CCA, since the water in the pipes has sufficient time to exchange heat with the concrete core such that their temperatures become equal. The simplified control approach therefore closely resembles current practice in real buildings, where the CCA return water temperature is tracked using a PI controller by modifying the CCA mass flow rate, we just make an abstraction of this mass flow rate control and assume that we have a sufficiently high inlet temperature to be able to achieve the heating curve set point. We verify the validity of these assumptions in the verification section of this deliverable.

Modifications of the primary system control for verification purposes

As mentioned earlier, the verification of the MPC model uses the detailed simulation model, since two algorithms can only be compared objectively if the same model is used for the comparison. The simplified controller is designed to be as close as possible to the detailed implementation such that the simulation model requires nearly no modifications. The main difference is that the CCA return water set point must be controlled to track the set point of the MPC approach, while the RBC approach uses a fixed return water temperature set point. A second difference is that the MPC approach assumes that the ventilation bypass is always closed. For consistency we apply the same assumption in the simulation model.

2.2. Design variables

The design variables for both approaches are similar, but not identical. First of all, the system sizes that have to be determined are the size of the 1) heat pump, 2) borefield, 3) boiler, 4) chiller and 5) FCUs.

The **heat pump size** is optimized by choosing a scaling factor. This scaling factor is multiplied with a 'best estimate' of the required heat pump size $Q_{hp,nom} = \Delta T c_p \dot{m}_{nom}$, which is computed by assuming that the heat pump has to be able to supply a temperature difference of ΔT=2K across the CCA at nominal conditions, i.e. at nominal mass flow rate $\dot{m}_{nom}$. The nominal flow rate is computed from the CCA surface areas and using a specific flow rate of 10 l/h/m². This heat pump size is multiplied by the scaling factor, which is the actual optimization variable. The scaled heat pump size determines a (different) scaling factor for the heat pump model, which has nominal performance data for 45 kW. Note that we need this best estimate in order for the algorithm to optimize within a realistic range, regardless of the building envelope size. I.e. we use the building surface area as a proxy for the heat demand of the building such that the algorithm tries realistic values for the heat pump size.

Similarly, the **borefield height** is optimized by letting the optimization algorithm choose a scaling factor, which is multiplied by a default borefield height. For determining this default height, we first compute the peak heating and cooling demand of the building envelope using a separate dynamic simulation. This peak thermal power is divided by the number of boreholes and a typical borehole thermal power of 30 watt per meter of borehole.

Each zone has its own **FCU**, for which a size must be chosen. We use performance data for the Jaga Briza 22 FCU, which fixes the ratio of the heating and cooling power that can be provided by the FCU for the chosen temperature regimes of 45 ˚C and 7 ˚C. Furthermore, we assume that a typical FCU sizing for a zone is 30 W/m² of zone surface area. Based on these values, the FCU size is computed for each zone, which is again rescaled using an optimization variable.

The **chiller** must be able to produce the total FCU cooling load, such that its nominal thermal power equals the sum of the FCU rated cooling powers. Similarly, the **boiler** thermal power equals the sum of the FCU rated heating powers.

2.3. Objective

The objective of this optimization is to minimize the net present cost[2] (NPC) of the system, which here consists of the investment costs in the system components that are subject of the optimisation and the operational costs for the building energy use for heating and cooling (that are also subject of the optimisation) for a period of 25 years. The energy costs are discounted over this period with a discount factor of 3% per year.

Investment costs

Both models use the investment costs that are summarized in Table 2 and that are expressed as a linear function of the component thermal power. The cost functions include the investment costs in the key component and their auxiliary components (pipes, fans, valves, collectors, expansion vessels etc.). These cost functions are based on research in task 2.5 and a detailed explanation can be found in D2.7. An exception is the FCU cost, which is based on publicly available catalogue prices for the Jaga Briza FCU, at 45 ˚C. Costs for CCA piping are not

[2] In this report, the net present cost is chosen as objective and performance indicator, as the optimisation focuses on the investment and operation costs for the system components involved. The net present value will therefore be >0, and the aim is to minimise it. An overall financial analysis of hybridGEOTABS buildings with RBC and MPC (taking into account the entire building costs, replacement costs, control costs etc.) takes place in WP4 and WP5, where the net present value (NPV) is used as a more complete indicator.

included in this exercise since they are not optimized; we assume that the full floor surface area is used to embed the piping. For the same reason, the investment cost in the MPC itself is not included.

Table 2: Investment cost data for the objective function per key component

Component	*Fixed cost [EUR]*	*Variable cost [EUR/kW]*
Heat pump	16194	163
Borefield	0	1000*
FCU	0	1000
Boiler	11700	105
Chiller	625	341

**Assuming 30 W/m and 30 EUR/m.*

Operational costs

In addition to the investment costs, we compute the operational costs for the energy use of the building. The main assumptions are that the chiller has a fixed COP of 3 and the gas boiler has an efficiency of 98 %. The heat pump has a temperature-dependent COP in the simulation model and a fixed COP of 7.5 for cooling and 6.75 for heating in the MPC model. These high COPs are based on the detailed simulation model results and are explained by the low temperature differences that exist in the hybridGEOTABS concept. Passive cooling using the borefield has a COP of 20 in the MPC model. We assume a fixed electricity tariff of 0.14 EUR/kWh and a gas price of 0.05 EUR/kWh, which is based on energy prices for commercial buildings in Belgium.

The model performs a 1-year simulation to compute the heat pump and chiller electrical energy uses and the boiler thermal energy use. This energy use is discounted over a 25-year period using a discount factor of 3 % per year. The total discounted cost over 25 years is returned by the model. The resulting geothermal heat load of the 1-year period is repeated 25 times in a separate simulation during which the ground temperature constraints are verified for the RBC approach. Similarly, the MPC approach repeats the geothermal heat load 25 times using the simplified geothermal borefield model and uses the resulting temperature response to compute the borefield supply water temperature limit penalty.

2.4. Constraints

Two soft constraints are implemented in the MPC model. Firstly, we constrain the zone temperature to 21 ˚C – 25 ˚C. Secondly, in order to avoid freezing the soil, we lower bound the supply water temperature towards the borefield to 2˚C. The maximum allowed injection temperature is 25 ˚C, which is 14.8 ˚C above the undisturbed ground temperature of Belgium (see Table 1). For other locations we therefore also set the upper limit of the supply temperature to 14.8 ˚C above the undisturbed ground temperature at the building location.

The RBC approach cannot enforce constraints. Therefore, they are considered using a pass/fail mechanism where too large constraint violations cause the design option not to be considered. For the remaining design options, the option with the smallest total cost is considered to be the best design option.

2.5. Technical implementation of the optimization algorithms

We now shortly summarize the implementation of the top-level optimization algorithm. This code is implemented using the python programming language. The algorithm loops over a set of building envelope models, which is an input for the algorithm, and 3 locations (Uccle, Madrid, Warsaw). The following actions are automatically performed for each envelope-location combination based on the user-defined set of allowed design options:

1. The required Modelica files are copied to a temporary folder such that multiple instances can run in parallel.
2. Custom Modelica files are generated that plug the envelope model in the above-described models. The interface between the envelope model and the HVAC model has been standardized to allow this. Any number of floors, zones and CCA sections is supported.
3. A simulation is run that computes the heat losses of the building. This model includes the building envelope, the ventilation system and an *ideal heating system* that maintains the zone temperatures at 23 ˚C. The resulting heat loss profile is used to estimate the borefield size.
4. An algorithm loops over all possible design options for the RBC approach, in each loop performing:
    a. A detailed simulation for the provided scaling factors and the default heating curve. Operational cost data (scaled for 25 years) and thermal comfort violations are collected from this simulation. Furthermore, this model saves the heat load of the borefield in a csv file.
    b. The resulting csv file is used in a separate model that only includes the borefield model to perform a 25-year simulation of the borefield. Borefield supply water temperature violations are collected from this simulation.
5. The MPC approach is run, which returns optimal scaling factors for heat pump, FCU and borefield, and heating curve.
6. These results are used to assess the real design cost using the more detailed 1-year simulation model. Operational cost data (scaled for 25 years) and thermal comfort violations are collected from this simulation. Furthermore, this model saves the heat load of the borefield in a csv file.
7. The resulting csv file is used in a separate model that only includes the borefield model to perform a 25-year simulation of the borefield. Borefield supply water temperature violations are collected from this simulation.

3. Model verification

Figure 2 illustrates that different models exist (RBC model and MPC model) that are solved using different Modelica tools (TADO, JModelica and Dymola). These models are now compared to each other to verify the implementation of the models. The main purpose of this comparison is to detect implementation errors in either of the two models and to provide an estimate of the modelling error. Note that all models respect conservation of energy up to high numerical precision. Each model is built up using components from the Modelica IDEAS library, which has been verified by Jorissen et. al [6].

3.1. Verification of TADO

Firstly, we compare the *MPC model* results using both TADO and the commercial Modelica simulation software Dymola. I.e. the MPC algorithm is first run to determine an optimal design of a test example. Once the optimal design is found using TADO, the optimal sizing is input for a simulation using the *same Modelica model*, in Dymola. TADO makes simplifications that increase the computation speed, which can cause errors. The main results are therefore compared to Dymola.

Results are summarized in Figure 4. This figure compares the results of the borefield supply water temperature, the total FCU cooling power (which equals the chiller power), the total FCU heating power (which equals the boiler power), the CCA thermal power (negative when heating), and the discomfort penalty that is used to penalize thermal comfort violations. We note small errors on the borefield temperature, which has slow dynamics and larger errors on the discomfort penalty and the FCU cooling power, which are linked to faster dynamics of the air temperature. These results are expected since fast dynamics are computed less accurately by the large time steps that we take. Larger errors can be seen for the FCU cooling power, however their integral values (i.e. the cooling *energy*) error is much smaller as can be seen in the next verification. These results are considered sufficiently accurate, especially since the more detailed model is used to compute the actual performance of the optimal design that is computed.

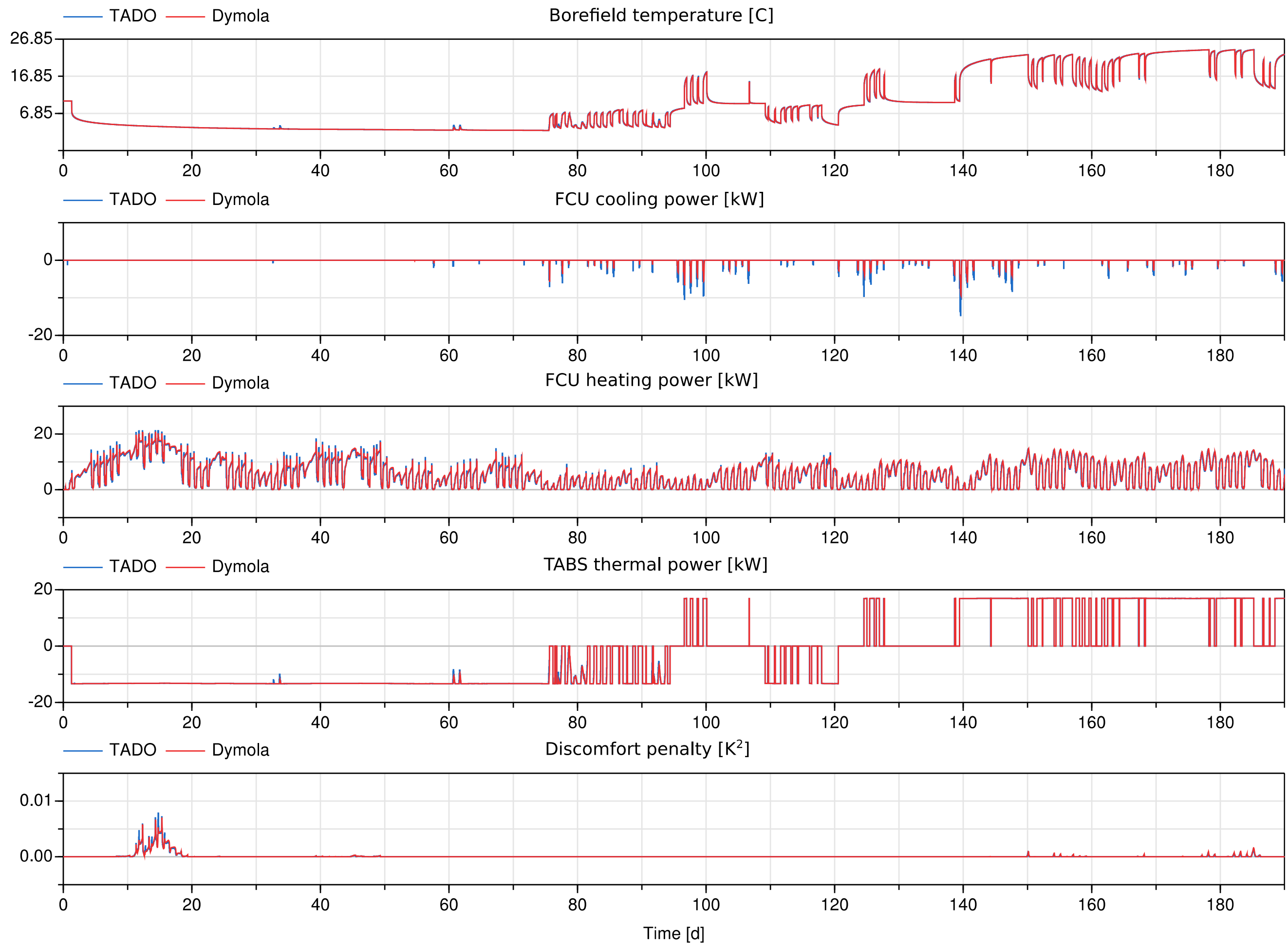

Figure 4: Comparison of optimization-based model results for Dymola and TADO

3.2. Verification of MPC model: building

Secondly, we verify the building (including HVAC) part of the MPC model, which is a simplified implementation of the RBC model. Furthermore, the results of the MPC model are injected in the more detailed model such that the model mismatch between the two models can affect the results of the overall approach in a negative way. We therefore compare the results of the MPC model to those of the RBC model. Starting from an optimal design, we perform both simulations using Dymola. Results are shown in Figure 5.

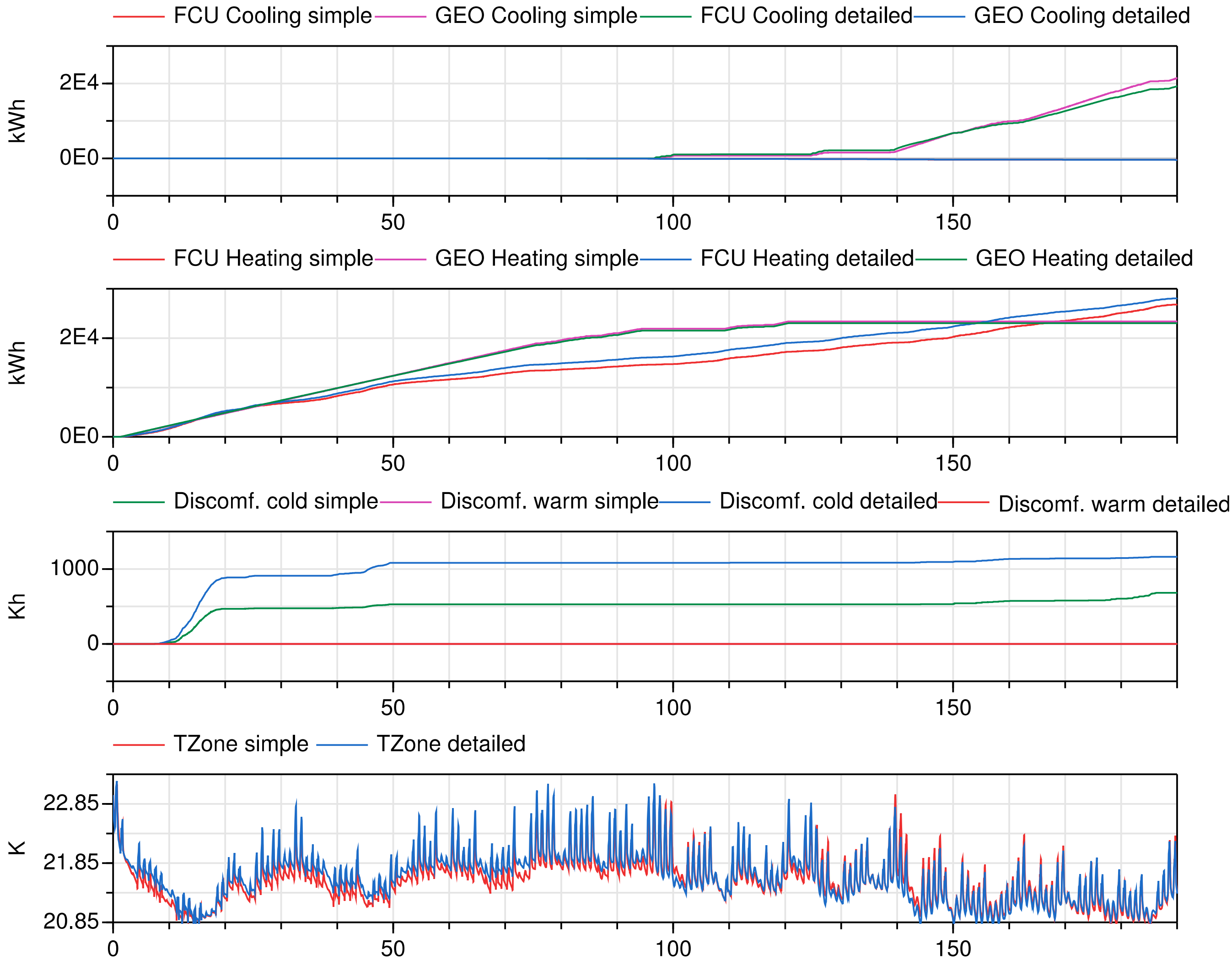

Figure 5: Result comparison for the building model between optimization model (simple) and simulation model using Dymola

All subplots show result differences, which are often relatively small, in the order of 10 %. The discomfort quantification error is larger, in the order of 100 %. This is because the MPC approach has small comfort constraint violations, which are easily doubled by model mismatch. Note that the indicated zone temperature is the result for one of eleven zones.

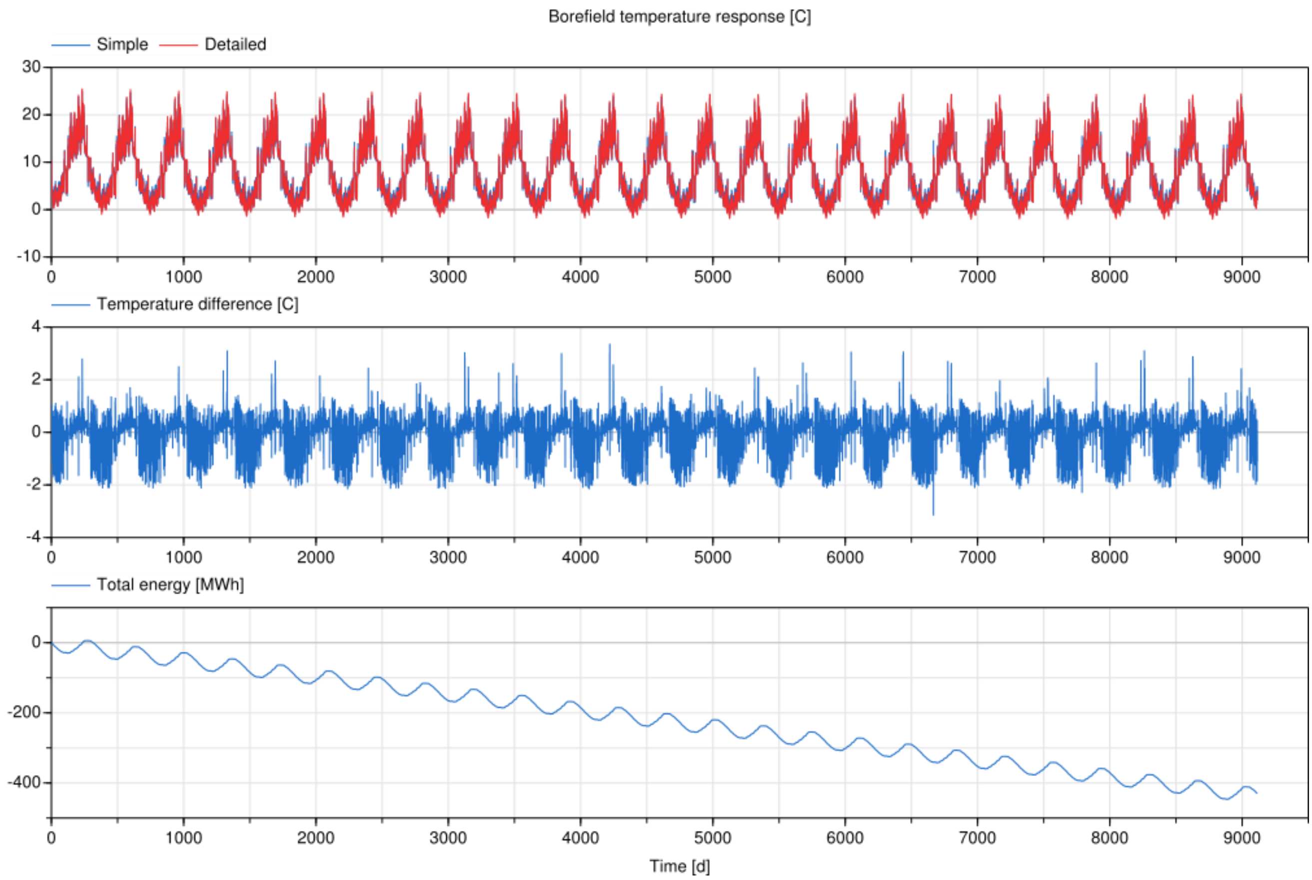

Figure 6: Result comparison for the borefield model between optimization model (simple) and simulation model using Dymola

3.3. Verification of MPC model: borefield

Finally, we verify the borefield part of the MPC model. To this end we store the thermal power profile of the borefield from the RBC model for a one-year simulation. We then reapply the same heat load profile to both the MPC and the RBC borefield model using Dymola and compute the supply water (towards the borefield) temperature response of both models. These temperatures are compared in the top subplot of Figure 6 and their difference is plotted in the middle subplot. The bottom subplot shows the total heat extraction from the borefield, which shows that a net heat extraction from the borefield occurs. This results in a temperature drop of about 1.2 K over the first years of operation. Since the borefield has relatively few boreholes, the temperature drop is limited. For larger borefields and lower soil thermal conductivities, a larger drop is expected. Note that the middle subplot shows no temperature drop, which indicates that the simplified model correctly predicts this temperature effect of the imbalance on the longer term. While the middle graph indicates that errors up to 2 K exist, the mean absolute error is only 0.38 K, which is considered acceptable compared to the temperature range of 25 K. Figure 7 shows the same result, albeit zoomed in on the last year.

We conclude that the presented models are sufficiently accurate for the purposes of this research. Some modelling errors clearly exist; however, these errors are not present in the final comparison of the different design options since all options are compared to each other using the more detailed simulation model. The model mismatch only affects the optimality of the found optimal result. This means that an increase in model accuracy can only improve the optimal result further. Given the small model errors, we however believe that this potential is small.

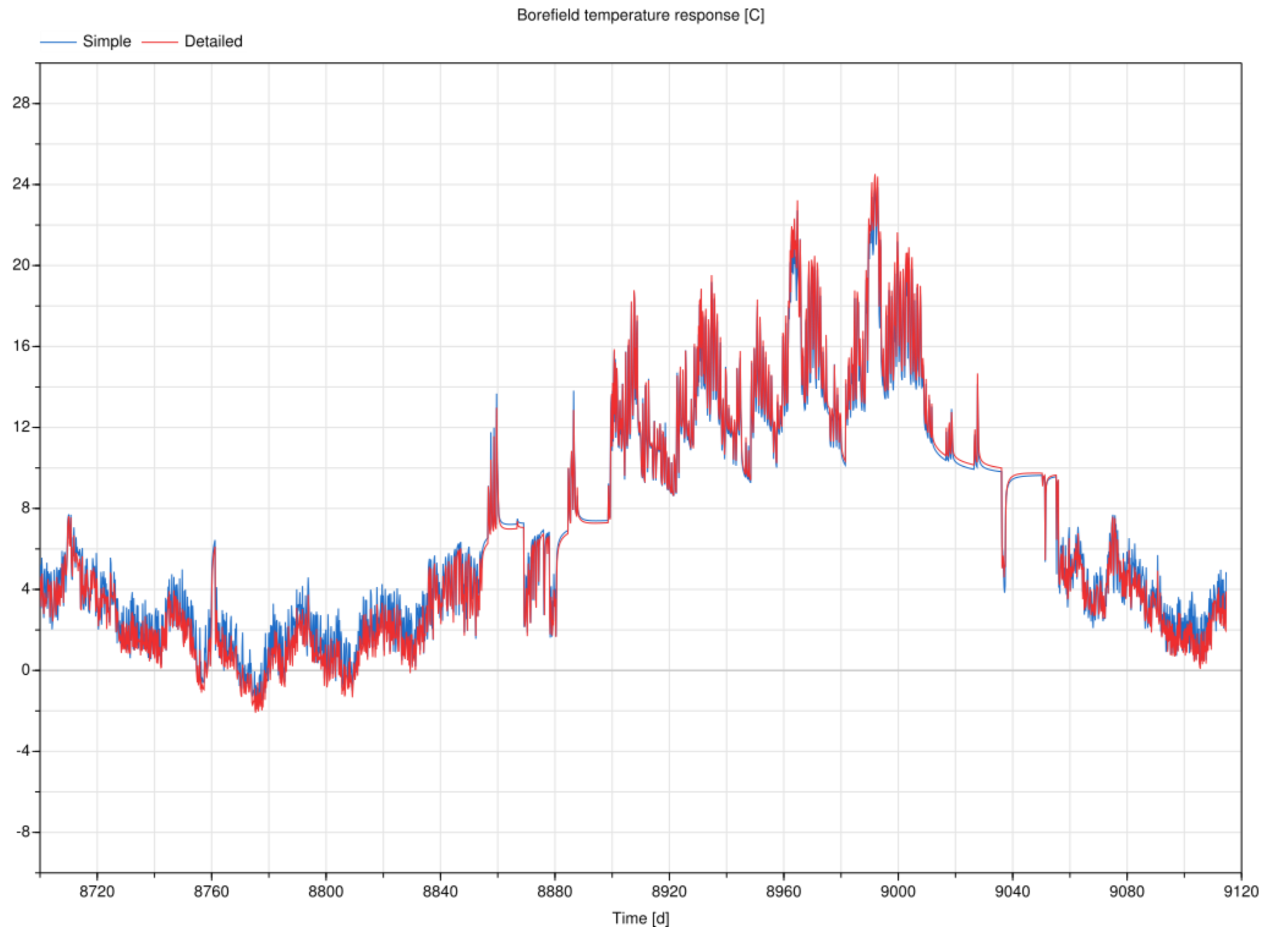

Figure 7: Result comparison for the borefield model between optimization model (simple) and simulation model using Dymola: zoom on year 25

4. Case-studies

4.1. Description of the selected case-studies

Geometrical form of the case study:

For this exercise we selected 9 cases from the building stock that is developed in the hybridGEOTABS project (D2.2 [7,8]). We choose one office building typology with a fixed geometry, and we varied the building physical properties such as the climate, thermal insulation and air tightness level, orientation, shading type and internal heat gains, which results in 9 different cases (see Table 5). The geometrical properties of the selected case are summarized in Table 3. To generate the building geometrical form in order to be used as an input for the building simulation tool Dymola, we applied a fitting process that is discussed in detail in deliverable 2.2 [7]. Figure 8 shows the archetype form and the input for the different variables that were used in creating the model.

Table 3: Office building case study geometrical properties

Geometrical variables	
Area [m²]	*2390*
Volume [m³]	*8532*
Heat loss surface area [m²]	*4325*
Height [m]	*6.4*
Number of floors	*2*
Window to wall ratio [%]	*38*
Compactness	*1.9*

Form dimensions	
a [m]	*15.5*
n	*2*
h1 [m]	*3.22*
L [m]	*57*
B [m]	*39*

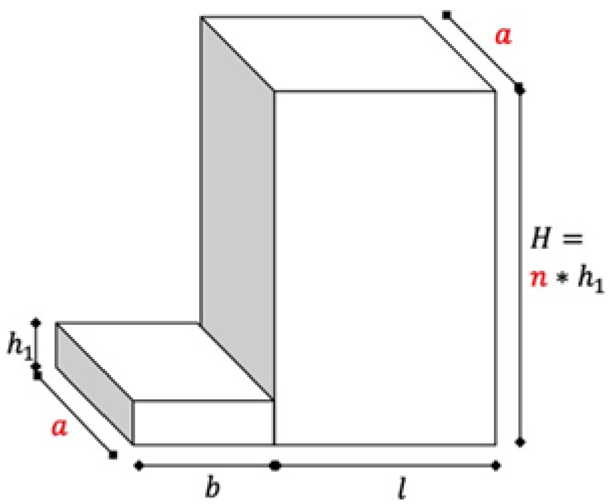

Figure 8: Building archetype general form and dimensions

Model description:

We used a multi-zone modelling approach for modelling and simulation of the case study. The building model has 2 floors with a total of 11 zones: each floor has 5 zones, and there is an attached zone to the building volume as shown in Figure 8. The building zones are divided based on typical office building functions such as: landscape offices, closed offices, a restaurant, meeting rooms and services zone as illustrated in Figure 9.

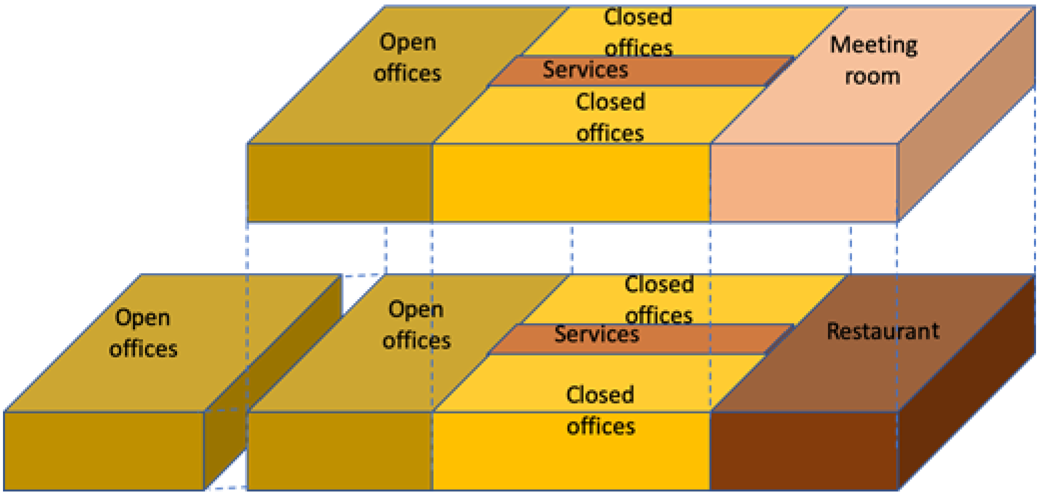

Figure 9: Office building model zoning

Building physical parameters:

Five building physical properties were varied in this exercise.

(a) Climate: We used three weather files that can cover most of the EU-different climates such as Brussels (Maritime, temperate warm), Madrid (continental subtropical) and Warsaw (transitional, temperate warm).

(b) Thermal insulation and air tightness level: we used three levels of thermal insulation of the building envelope and windows as well as the air infiltration rate, summarized in Table 4. The three groups were decided based on the current regulations and codes for buildings in the different EU countries. Setting (1) represents a building with lower thermal transmission and high airtightness according to the passive house standards, setting (2) represents a building with average thermal transmission and airtightness according to today's energy performance regulations observed in many EU countries, and setting (3) represents a building that has higher thermal transmission and lower airtightness as observed in some Mediterranean regulations today and older buildings.

Table 4: Three different categories that represent the building energy performance regarding the building envelope and airtightness

	U-value opaque [W/m². K]	U-value windows [W/m². K]	Airtightness at n50 value 1/h
High	0.15	0.80	0.6
Medium	0.27	1.5	2.0
Low	0.50	2.5	5.0

(c) Occupancy profiles: we identified two categories for internal heat gain profiles in offices based on the office density, such as low dense office and high dense office. The internal heat gains dynamic profiles account for occupancy, lighting and vary throughout the day and week. For the low dense office, the internal heat gains are on average 18 W/m², and for a high dense office on average 33 W/m².
(d) Shading system: We choose two options, either buildings with window shading system where an external screen is controlled for all windows. The external screen goes down (on) when solar irradiation on external windows exceeds 150 W/m². The second option is the use of no shading system.
(e) Orientation: We choose two orientations, west or south, where the largest facade is either facing the west or the south directions.

The 9 cases that were selected are summarized in Table 5 and are a reflection of the variety of cases in the building stock in T2.2. Note that not all these cases are equally likely to occur in practice. E.g. the low insulation group C is more likely to occur in the warmer regions of Europe in new buildings and using them in colder climates will cause a significant heat demand, for which low temperature emission systems such as TABS are less suited.

Table 5: Summary of the 9 cases regarding the different parameters that are varied

Group	Climate	Thermal insulation group	Occupancy	Shading system	Orientation
[A]	Brussels	Medium	Low-dense	yes	South
	Madrid	Medium	Low-dense	yes	South
	Warsaw	Medium	Low-dense	yes	South
[B]	Brussels	High	High-dense	yes	South
	Madrid	High	High-dense	yes	South
	Warsaw	High	High-dense	yes	South
[C]	Brussels	Low	High-dense	No	West
	Madrid	Low	High-dense	No	West
	Warsaw	Low	High-dense	No	West

4.2. Heating and cooling demands of the case-studies

In order to introduce the energy-related behaviour of the case-studies, the total yearly heating and cooling demands are presented, providing insight in the amounts of energy the building would require to maintain thermal comfort, to observe the balance between heating and cooling etc. To obtain the heating and cooling demands of the building, the building envelope model, explained in previous section, is coupled to an ideal heating and cooling system. The ideal heating and cooling system maintains the thermal comfort by giving/receiving energy to/from the building as much as needed to keep the temperature of different zones in the building between 22°C and 24°C. The hourly demand is calculated for all the year. Then, to have the load duration curves, the hourly demands are sorted from the maximum to the minimum value (zero). By that, the maximum value, the behaviour of the load, and the thermal (im)balance are recognised from the graph. The cooling demand is shown in negative numbers to be separated from the heating demand for increasing the readability of the graphs (Figure 10). Figure 11 presents the total annual heating and cooling demands.

The highest energy use for heating and cooling is observed in the cases C, that are the cases with the lowest insulation and airtightness levels. These buildings are very susceptible to climatic conditions (temperature, wind and solar gains) and to high internal gains. The cases A have a more typical or average insulation and air tightness level and a less dense occupation and shading, which will lead to considerably lower fluctuations in heating and cooling demands than in cases C. Logically, in Madrid, all cases C and A are cooling dominated, while in Brussels and Warsaw the cases are heating dominated. Finally, the cases B are highly insulated and shaded – similar to passive houses – but have a high dense occupation. This results on one hand in a very low heating demand (also in Brussels and Warsaw), but also in considerable cooling demands, to compensate for the high internal heat gains that are 'trapped' in the heavily insulated building.

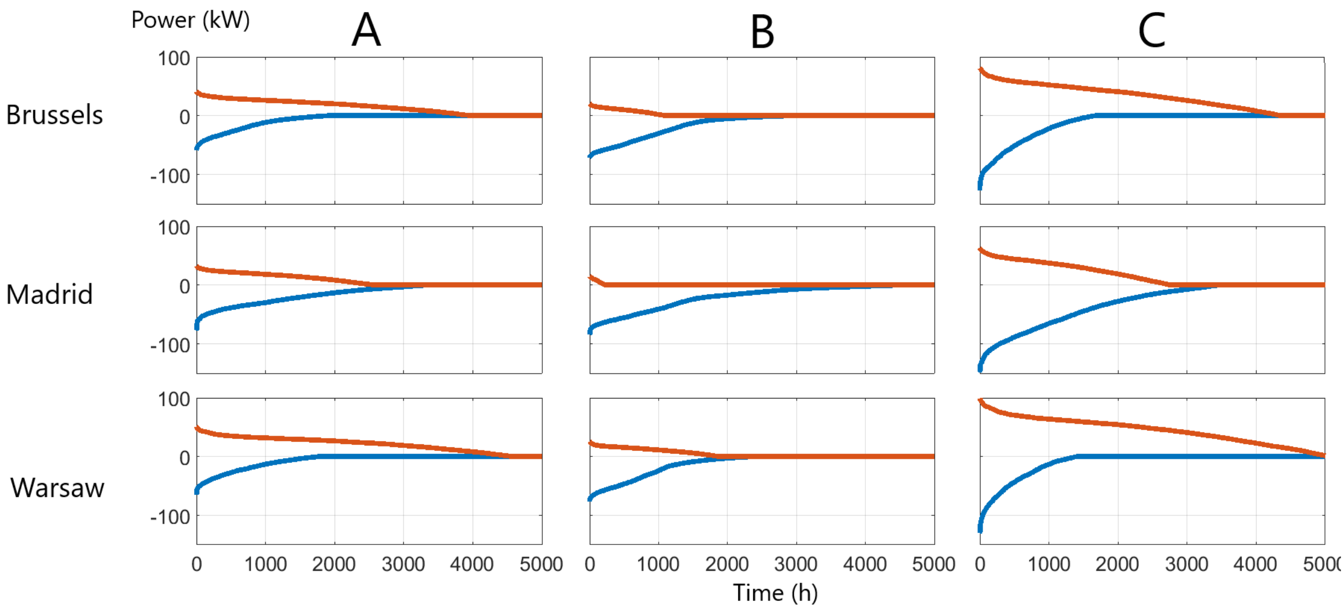

Figure 10: Load duration curves for all 9 cases

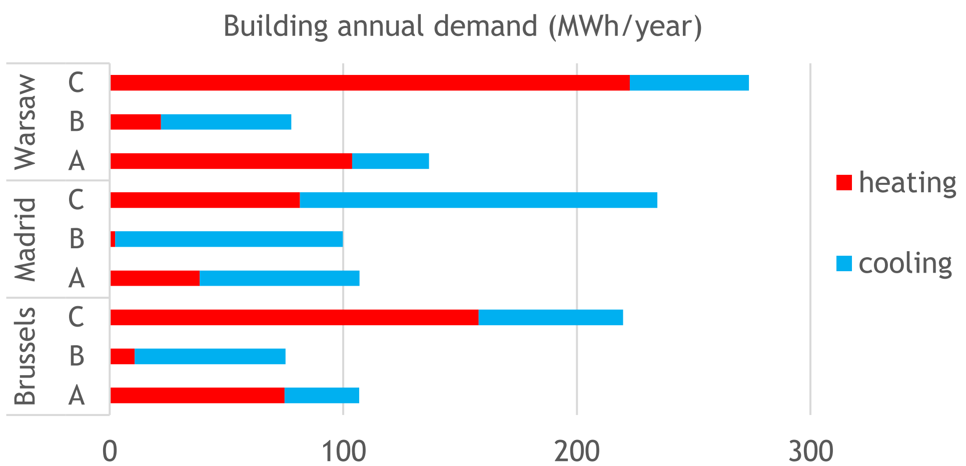

Figure 11: Building annual heating and cooling demands for 9 cases

5. Comparison between results of RBC and MPC

By comparing the RBC-approach and MPC-approach (introduced in section 2), we can estimate the effect of applying a (near-)optimal control-integrated HVAC design with MPC (the MPC-approach) as compared to a good sizing with current practice RBC (RBC-approach). The main performance indicators that are decisive in early design stages are the financial costs (investment and operating costs) and the environmental performance of the HVAC-concept. The main parameters that are varied are the size of the key primary and secondary HVAC-system components, and the share of the building heating and cooling demands that can optimally be covered by the primary and secondary system[3]. This share is not only influenced by the size of the components, but also by the control algorithm. This is why the control is considered already when deciding on the size of the components. When comparing RBC and MPC, the main performance indicators observed are thus: the net present cost (NPC), CO_2-emissions, energy use (load splitting) and sizing of the components.

In this section, the main performance indicators are estimated for both the RBC- and MPC-approaches, by applying them to the case-studies. The RBC-approach is essentially a brute-force optimization algorithm that tries all design option combinations. In order to limit the set of design options to a computationally feasible set, the allowed design sizes were chosen as follows (see also section 2.2):

- the allowed heat pump sizes are 100%, 70% and 40% of the 'nominal' size
- the allowed borefield sizes are 100%, 75%, 50% and 30% of the nominal borefield size
- the allowed FCU sizes are 75%, 50% and 30% of the nominal size of 30 W/m^2.

While the RBC-approach has a discrete set of design choices, the MPC-approach can choose any real value between 10% and 100% for the FCU and HP size, and any value between 10% and 300% for the borefield size. Note that a size close to the industry standard sizing was chosen as the upper sizing limit to ensure that computation time does not explode because of a too large set of design choices.

As introduced in section 4, the case-study buildings are office buildings in three EU-climates (Madrid, Brussels and Warsaw), with 3 types of building physical properties (A, B, C). For each of them different combinations of design options (sizes) of the key components are tested for both the RBC- and MPC-approaches. As a result, the outcomes for 5 cases are presented in the next sections. For 4 out of 9 cases no satisfactory design[4] could be identified for both the RBC-approach and the MPC-approach. These four cases consist of the three cases in group C (Brussels C, Madrid C and Warsaw C) and case Warsaw A. The C-cases combine relatively low insulation levels (and thus relatively higher heating and cooling demands) with high internal gains, and thus high sudden variations in demand that are typically covered by the secondary system. Therefore larges system sizes would have been required to satisfy the demands. For case Warsaw A similar reasoning applies. Note that this result does not rule out hybridGEOTABS, nor the optimisation approach, for these specific cases. On one hand, a hybridGEOTABS solution for those cases would consist of relatively larger secondary systems and a relatively smaller share of GEOTABS, as can be seen from the results in D2.5-D2.6. On the other hand, in a good building design practice, the architect and HVAC-designer have the freedom to choose the most suitable combination of building physical (and sometimes also building geometrical) properties to allow a high share of GEOTABS. The design tool presented in D2.6 assists the designer in making this decision.

---

[3] The designer, or the design optimisation algorithm, stands for the choice to either increase the primary GEOTABS-system size, either increase the secondary system size in the search for an optimal financial and environmental solution, that allows to meet the heating and cooling demands required to reach thermal comfort in the building.
[4] A satisfactory design needs to maintain thermal comfort (< 100 Kh of comfort violations per year) while at the same time maintaining the borefield temperature between the allowed temperature limits (< 1000 Kh per year).

5.1. NPC and CO_2-emission

The net present cost (NPC) is used as financial performance indicator. As explained in detail in section 2.3, the objective function minimises the net present cost, that accounts for the investment cost and the energy costs during operation for a period of 25 years. The environmental performance is indicated by the CO_2-emissions, that are calculated by using CO_2-conversion factors for the EU in 2020, in line with the definition and motivation in deliverable D5.3. The CO_2-conversion factor for electricity is 260 g/kWh and for natural gas it is 220 g/kWh. In Figure 12 the NPC and CO_2-emissions are presented for the 5 cases.

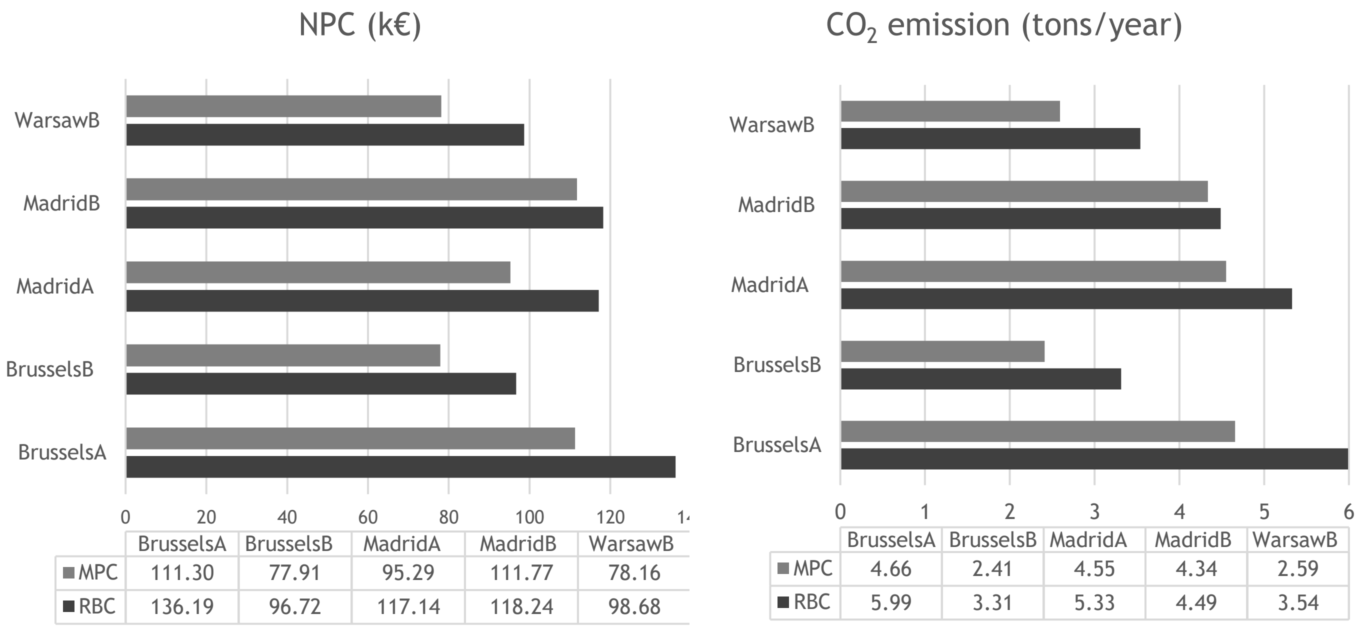

	BrusselsA	BrusselsB	MadridA	MadridB	WarsawB
MPC	111.30	77.91	95.29	111.77	78.16
RBC	136.19	96.72	117.14	118.24	98.68

	BrusselsA	BrusselsB	MadridA	MadridB	WarsawB
MPC	4.66	2.41	4.55	4.34	2.59
RBC	5.99	3.31	5.33	4.49	3.54

Figure 12: NPC and CO2-emissions for 5 cases with RBC (bottom) and MPC (top) approach

The results in Figure 12 clearly indicate that for all 5 cases the NPC decreases with 5 % to 20 % and the CO_2-emissions decrease with 3 % to 28 % when using MPC instead of RBC. Looking deeper into the individual cases (see also Table 6), the highest reductions are observed for Brussels B and Warsaw B. Then Brussels A and Madrid A have reductions of about 18% in NPC and 22% and 14% respectively in CO_2-emissions. Finally, the Madrid B case gains least from the MPC-approach, with reductions in NPC of 6% and reductions in CO_2-emissions of 3 %. This case is very well insulated and received high internal gains both due to occupancy and solar gains, and as a result has negligible heating demands, but significant cooling needs. In order to better understand the reasons for these differences, also the thermal balance, peak and annual demands, sizing of the key components etc. need to be looked into. In the next step, the costs for each scenario are split out per system component, thus giving an indication of sizing differences between the various scenarios.

In Figure 13, Figure 14 and Table 6 the NPC is split into investment costs (hatched) and operating costs for a period of 25 years[5]. The costs related to the primary GEOTABS system are in green colours while the other colours refer to the secondary system related costs. When comparing RBC and MPC results for each case-study, the total NPC reductions are due to both reductions in investment and operation costs.

[5] The costs are subdivided according to the sub-systems (primary and secondary production and emission systems for heating and cooling) and are named after the key components of these sub-systems. Therefore, for each key component, the investment costs includes also the 'auxiliary' components of the sub-system (see also section 2.3).

With the MPC approach the investment cost for the heat pump and the boiler are always lower than the RBC approach. However, this reduction is not substantial since both components have a large fixed cost (see Table 2) and therefore their size reduction will not show itself clearly in the investment costs. On the other hand, the fan coil unit and the chiller investment cost reductions are obvious and decisive, and go together with a decrease in the operating costs for the fan coil unit in both heating and cooling. The geothermal borefield is, together with the heat pump, responsible for a significant part of the investment costs. When going from RBC to MPC, the borefield cost increases for 3 out of 5 cases, as the MPC uses the primary system more. This however is not per se translated into a higher operation cost of the primary system, as the improved control of the MPC leads to a more efficient operation in 4 out of 5 cases (and only a small increase in the remaining case). These results demonstrate the importance of system integration, with a crucial role for the controller as system integrator. Minimizing towards total cost cannot be directly translated in a size reduction for all system components.

Table 6: Decrease (+) or increase (-) in costs when using MPC-approach instead of RBC-approach for 5 cases (in % of total NPC).

		BrusselsA	BrusselsB	MadridA	MadridB	WarsawB
Investment costs	Heat Pump	1.3	0.9	0.6	3.0	0.5
	Boiler	0.7	0.8	0.7	0.1	0.8
	FCU	6.2	7.8	6.9	1.4	7.6
	Chiller	2.8	3.6	3.2	0.6	3.5
	Borefield	1.3	-2.4	3.2	-0.6	-1.6
	Total reduction	12.3	10.7	14.6	4.5	10.8
Operating costs	Heat pump	1.8	3.0	-0.4	0.7	5.1
	FCU Heating	2.6	0.2	1.8	0.2	-0.6
	FCU Cooling	1.6	5.6	2.7	-0.1	5.6
	Total reduction	6.0	8.8	4.1	0.9	10.0
Total NPC reduction		18.3	19.5	18.7	5.5	20.8

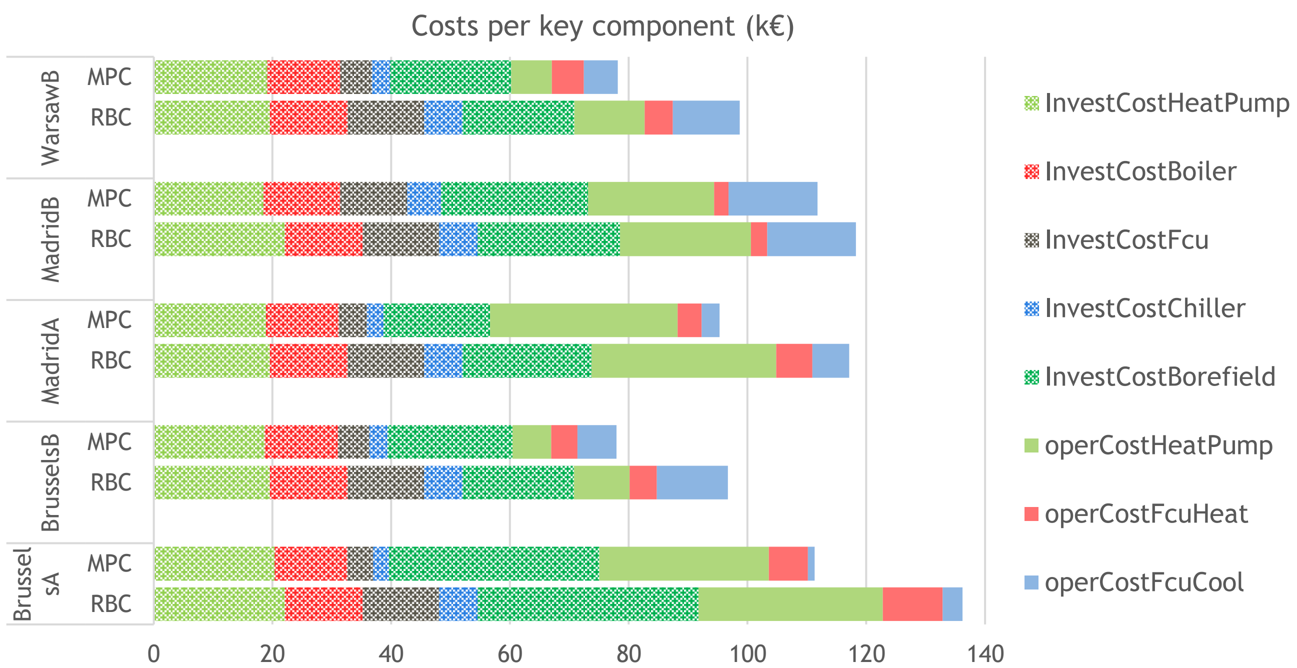

Figure 13: NPC costs per key component for 25 years, comparing RBC and MPC approach for 5 cases

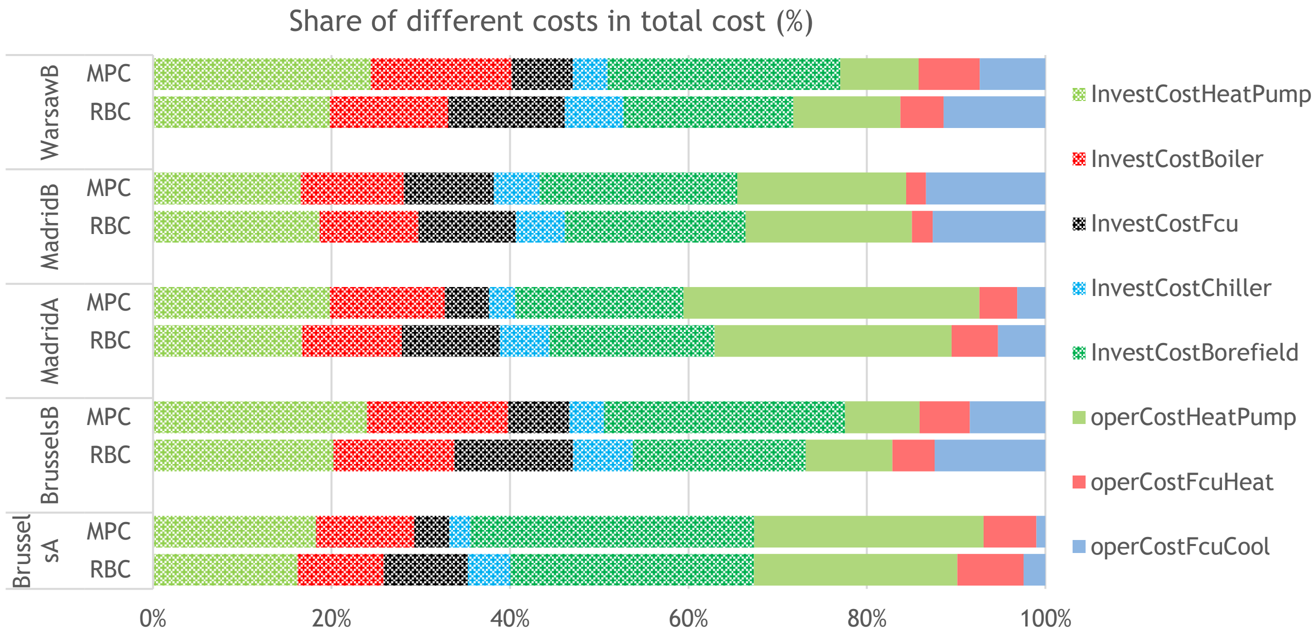

Figure 14: NPC per key component for 25 years, comparing RBC and MPC approach for 5 cases (% of total NPC)

Of course, each case-study has its own specific characteristics, and some designs may be more appropriate for allowing high shares of GEOTABS than others, or they are simply more appropriate for their given climatic and use conditions. In the introduction of section 5, this was already explained for the 4 cases that are not included in the results. For the 5 cases with results, for example, a passive house building envelope design (group B) is more suitable for hybridGEOTABS buildings in colder climates like Brussels and Warsaw, than it is in warmer climates like Madrid. In the Madrid climate, the high insulation levels, here combined with high occupancy, lead to a minimisation of heating demands and increase in cooling demands (often with higher and more sudden variations), thus reducing the balance between heating and cooling that is important for maintaining the temperature balance in the borefield, and increasing the need for the secondary system (see also Figure 17), and reducing the saving options of the MPC when compared to RBC. In general, for all 5 cases going from RBC to MPC has its benefits, but for the more appropriate designs, the gains are more pronounced. Conservatively and based on these 5 cases, we can conclude that the optimisation leads to a decrease of the investment and operating costs of the secondary system, combined with an increased use and more efficient operation of the primary and more environmentally friendly system.

5.2. Energy use (load splitting)

The energy use is investigated at two different levels. On one hand, the building energy use is the heating and cooling delivered to the building zones by the emission systems for realising thermal comfort throughout the year (as explained in section 4.2). In this case, the heating and cooling generation and distribution system efficiencies are not considered. This energy use is represented in Figure 15 for the RBC-approach and the MPC-approach, in which the heat is released or absorbed from the building by using TABS and FCU as emission systems. It is also compared to the case in which an ideal heating and cooling system would be used and provide indoor temperatures between 22°C and 24°C (similar to the temperature objectives of the MPC and RBC approaches). It is observed that the TABS may lead to an increase or decrease of the energy use at the emission system level.

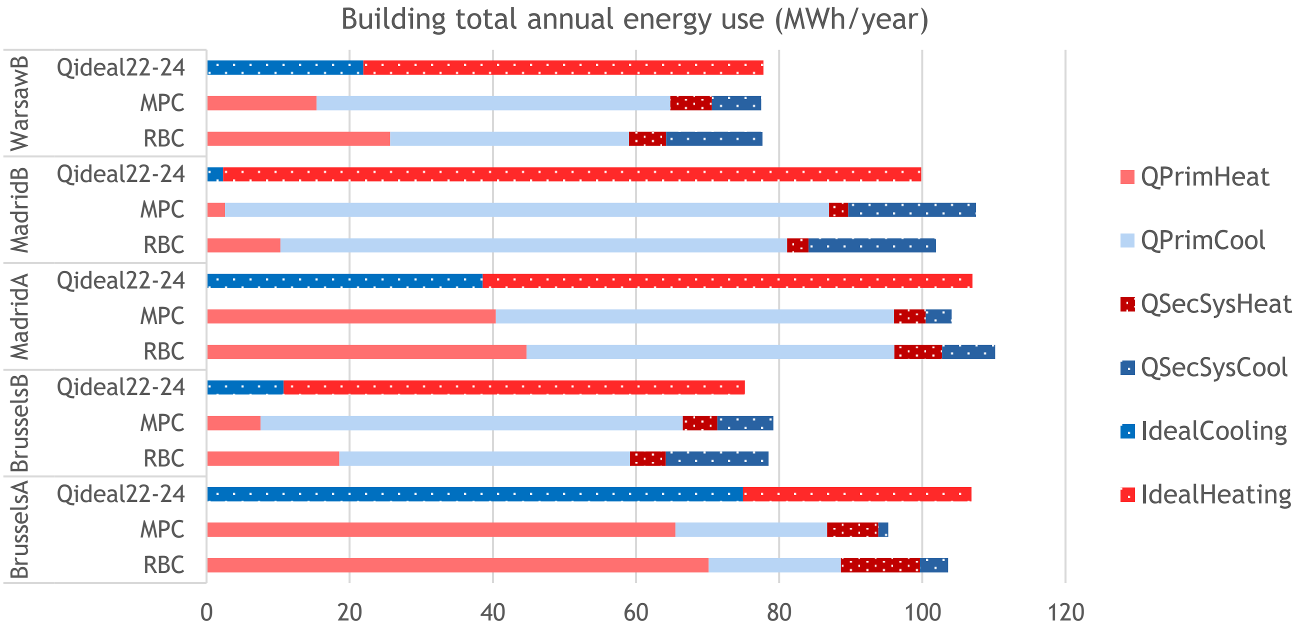

Figure 15: Annual energy use with the RBC and MPC approach for 5 cases

On the other hand, in Figure 16 the primary energy use of the systems is observed, taking into account the efficiencies of the entire system and the conversion to primary energy. In the end, this primary energy is what really counts when talking about building energy performance. The comparison between RBC and MPC shows a reduction between 3 % to 26 % in primary energy use for the 5 cases. Remark that the building total annual energy use (in Figure 15) can be higher for MPC then RBC (e.g. in Brussels B and Madrid B), but the overall primary energy use is significantly lower, as the primary GEOTABS system has a higher efficiency.

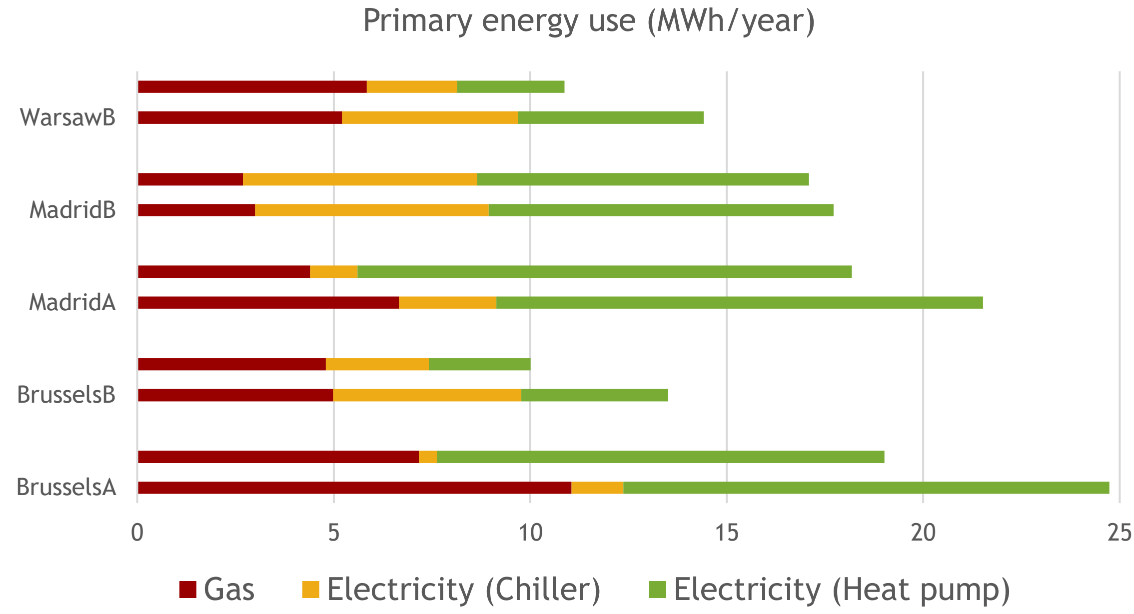

Figure 16 : Primary energy use with the MPC (top) and RBC (bottom) approach

In order to look at the general behaviour of the MPC approach when compared to the RBC approach, in Figure 17 the building annual energy use for the primary and secondary systems in heating and cooling are expressed as % of the total building annual energy use per scenario, and so the share or load splitting between the primary and secondary system is presented. It is found that the overall share of the GEOTABS system is higher than 75% of the energy use in all 5 cases. The optimisation done by the MPC approach leads to an increase in the share of the primary system for all cases, up to 10% in some of them. The highest share is seen in Brussels A, and accounts for 90% of the energy use. Looking back at the primary energy use figures, it is seen that a significant part of the primary energy use (due to the secondary systems) originates from a very small part of the energy emitted to the building zones.

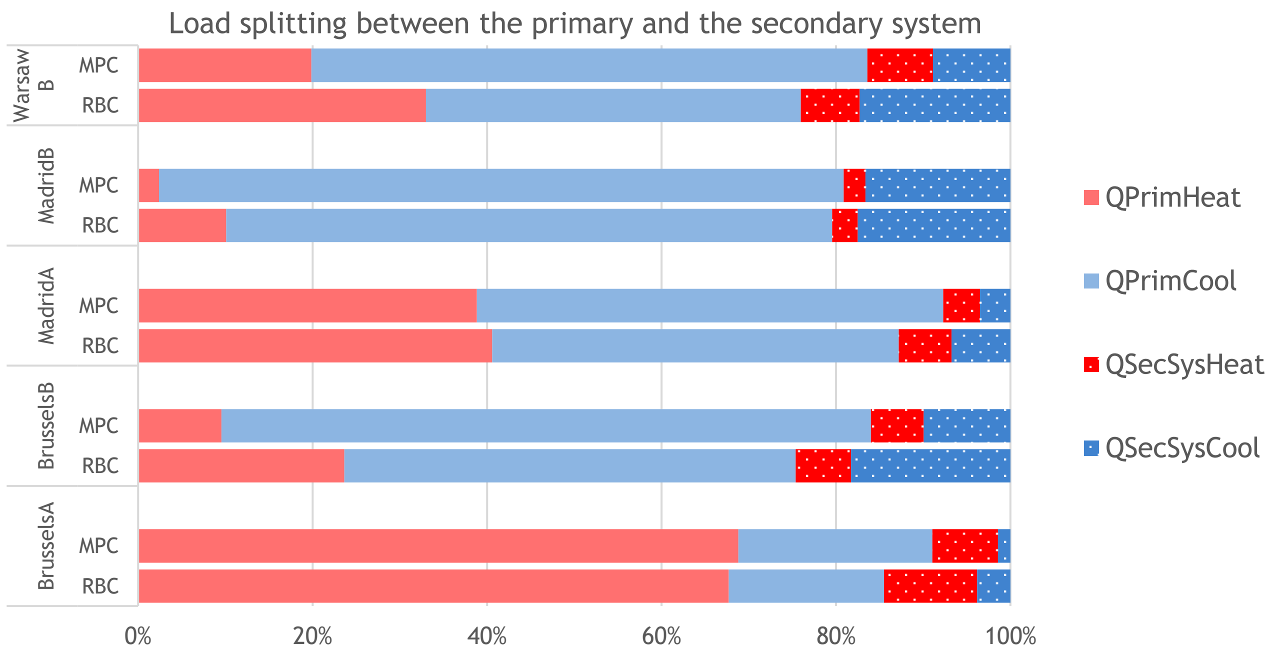

Figure 17: the shares of the primary and the secondary system in heating and cooling energy use with RBC and MPC approach for 5 cases

5.3. Key Component Sizing

The changes in investment costs between RBC and MPC approaches are a result of the changes in sizing of the key system components, but as the costs consist of fixed and variable costs, the change cannot directly be translated to component sizing, so from a technical point of view it is worth to also observe the component sizes. The key components of the primary GEOTABS system are the TABS, the heat pump, the ground source heat exchanger or geothermal borefield, and the Model Predictive Controller [9,10]. In pre-design stage the TABS sizing is not a critical aspect: it is assumed TABS is installed in 80% of the conditioned floor area of the building. The heat pump and borefield are the key components influencing the costs. For the secondary system, in this study considered as fan coil units coupled to a chiller and gas boiler, the size of the boiler and chiller are analysed (and FCU depend on their size). The power of the energy conversion components is therefore presented in Figure 18, and the size of the GSHX is expressed in Figure 19 in terms of the total length of the borefield. Apart from the results of the RBC- and MPC-approach, Figure 18 also presents the design power (Q_{design}) for heating and cooling of the case-study buildings as obtained by more traditional HVAC design practice, where the total installed power is based on a classical steady-state heat loss calculation at the critical design days for heating and cooling (methodology as explained in D2.6 and D2.7).

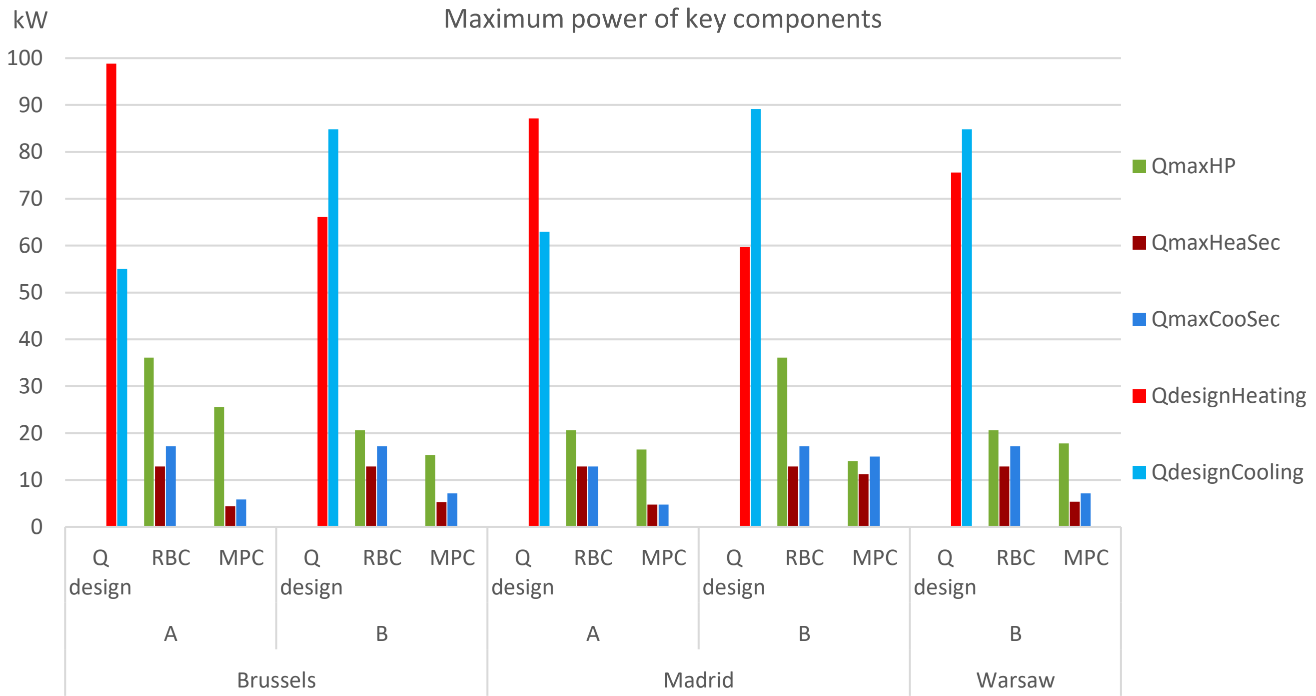

Figure 18: Comparison between size of different components with different approaches for 5 cases

When comparing the design power Q_{design} in heating to the sum of powers of the heat pump and the gas boiler, the hybridGEOTABS sizing leads to a reduction of heating power between 18% and 62% with RBC and 58% to 76% with MPC. The smallest reduction of 18% is observed for the case Madrid B with RBC, as the rather large heat pump size is actually required for its cooling function. Regarding the cooling power[6], reductions between 16% and 60% are observed for RBC and 52% to 77% for MPC when comparing to Q_{design}. Also here, for example the small reduction in Brussels A is because of the heat pump size that is dominated by heating requirements.

[6] The cooling power in the hybridGEOTABS scenario's is estimated by adding the power of the chiller to 80% of the power of the heat pump (as cooling power is about 20% lower than heating power for the same heat pump). Remark however that part of the cooling demand is realised by passive cooling rather than active cooling, especially in moderate and cold climates.

The significant reductions in heating and cooling power obtained by the hybridGEOTABS sizing, illustrate the need and the value of an integrated sizing methodology for hybridGEOTABS systems. The reason behind these reductions is that the buffer capacity of TABS has the ability to store the energy, and by spreading the (lower) power over a large time period, smaller production units are achievable and peak shaving is possible. Also, as discussed more in depth in D2.5, the critical design days used in classical steady-state heat loss calculation methods are not per se the most critical for sizing primary and secondary hybridGEOTABS systems. This emphasizes the importance of having a specific design methodology for hybridGEOTABS rather than using methods which are used for conventional systems.

Comparing the component sizes for RBC and MPC, for each of the 5 cases, the sizes of the heat pump, chiller and boiler are smaller with the MPC approach than with the RBC approach. The heat pump power decreases with 13 % to 60 % when using the MPC approach, which is a significant size reduction. However, as mentioned before, this has only a limited influence on the investment costs: a power reduction of about 50% can only reduce the price of the heat pump investment with about 10%, and the total cost with about 2%. The power of the boiler and chiller reduce between 13% and 66%.

Finally, Figure 19 compares the size of the borefield in different cases under the two different approaches. As seen, the total length of the borefield in cases B increases by using the MPC approach. While, in the cases A, the size of the borefield is smaller when the MPC approach is used. When comparing to Figure 15, indeed in the cases B the primary system delivers more energy to the building in the MPC case than in the RBC case, and vice versa for the cases A. As mentioned before, a good sizing of the borefield is an important aspect of the hybridGEOTABS system design and competitiveness, as the borefield cost can be up to 35% of the total HVAC-costs. However, the optimisation exercise with MPC shows that even for the cases with a larger borefield, the overall NPC and CO_2-emissions decrease.

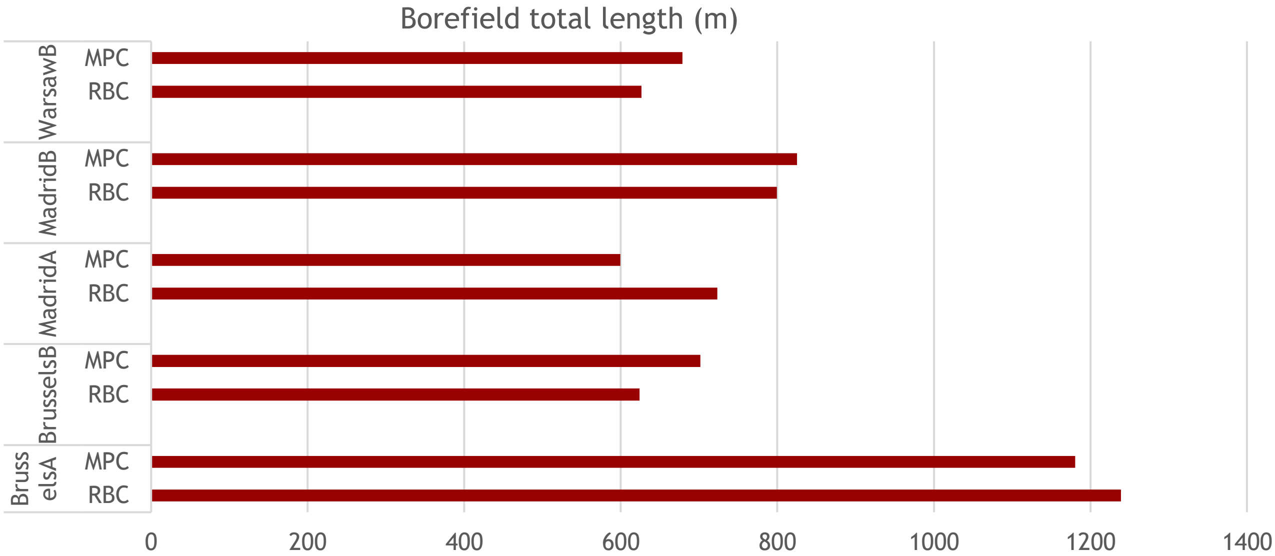

Figure 19: Borefield length with RBC and MPC approach for 5 cases

6. Conclusions

In this report, the sizing and performance of the (near-) optimal hybridGEOTABS HVAC design with MPC (the 'MPC-approach') is quantified and compared to those obtained by selecting the best design solution with a current practice RBC (the 'RBC-approach'). It is concluded that by using the MPC-approach, the optimisation leads to a reduction in the net present cost of the HVAC-system, and a reduction of the environmental impact as indicated by the CO_2-emissions and primary energy use. The values are case-dependent, and for the cases in this study the reductions go from a few percentages up to significant reductions of 20% for the NPC, 28% for the CO2-emissions and 26 % for the primary energy use.

Behind these numbers, throughout the cases a consistent tendency is observed: the control-integrated optimisation (the MPC-approach) leads to a decrease in the size and investment cost for the secondary HVAC-system together with a reduced energy generation and operating costs. This reduction of the secondary system goes together with an increase in the amount of energy provided by the GEOTABS system to the building (which aligns with a similar or increased size of the geothermal borefield), combined with a significant reduction (between 13% and 60%) in the heat pump size due to the more efficient MPC control. In conclusion, the hybridGEOTABS system MPC-integrated design leads to an increase in the use of GEOTABS (to more than 80% of the overall heating and cooling energy use of the building in the cases studied) which is beneficial from both financial and environmental point of view.

Additionally, the total (primary and secondary) heating and cooling powers in the hybridGEOTABS designs, are significantly - up to more than 70% - lower, than the powers obtained in classical HVAC design practices that rely on steady-state heat loss calculations for a critical design day. The use of these classical practices would evidently lead to higher investment costs as well, and reduce the feasibility of hybridGEOTABS. This illustrates the need and the value of an integrated sizing methodology for hybridGEOTABS systems, as the one developed in this work package 2, that takes into account the properties of TABS, the interactions between primary and secondary systems and the control as system-integrator.

Final note: situation of this work in the development of a hybridGEOTABS design methodology

The development of a design strategy for optimal sizing of hybridGEOTABS system components in feasibility and pre-design stage, is the main objective of this work package (WP2). The approach to come to this design methodology includes the building energy simulations of a large amount of building cases from the EU building stock (T2.2), the use of a computationally fast load splitting algorithm (T2.1) and post-processing of its outcomes to come to a sizing of the key hybridGEOTABS system components (HP (&TABS), GSHX, SS) for a variety of cases appearing in the EU building stock (T2.4-2.5). To arrive to this computationally fast strategy, the use of simplifications is inevitable. One such simplification is the level of detail in which the HVAC-systems and controls, and their interaction with the building, are dealt with in the T2.1 baseload splitting algorithm. Therefore, in this task (T2.3), that aspect is studied more in detail by using (some of) the same cases as in the building stock modelling. The findings from this study on a limited amount of case-study buildings are used in the subsequent tasks of this work package in an additional validation (in D2.5-6-7) of the more simplified and computationally faster design strategy that is based on the application of the baseload algorithm [11,12], that also integrates control-aspects in the design albeit in a more simplified way, and the building stock simulation results.

List of Tables

List of Figures

Bibliography

[1] O.B. Kazançi, D. Khovalyg, B.W. Olesen, Q. Wang, S. Dag, A. Caminade, J. Hoogmartens, J. Cigler, G. Parnis, W. Boydens, H. Cano Esteban, F. Cordero Tosal, J. Borrajo Bastero, E. Himpe, J. Laverge, D6.1 hybridGEOTABS system concept: document defining the system concept, individual modules and interfaces, in: HybridGEOTABS Project (H2020-Project MPC-.GT), Danish Technical University, Kopenhagen, Denmark, 2020. http://www.hybridgeotabs.eu/publications/deliverables.

[2] I. Cupeiro Figueroa, D. Picard, W. Boydens, G. Parnis, L. De Backer, D4.5 Report describing the two baseline cases: nonGEOTABS-RBC and hybridGEOTABS-RBC, in: HybridGEOTABS Project (H2020-Project MPC-.GT), KU Leuven, Leuven, Belgium, 2017. http://www.hybridgeotabs.eu/publications/deliverables.

[3] F. Jorissen, L. Helsen, D2.3 Software code representing nested optimisation algorithm, leading to optimal design that integrates optimal control, in: HybridGEOTABS Project (H2020-Project MPC-.GT), KU Leuven, Leuven, Belgium, 2019. (confidential).

[4] M. Cimmino, M. Wetter, Modelling of Heat Pumps with Calibrated Parameters Based on Manufacturer Data, in: Modelica Association and Linkoping University Electronic Press, Prague, Czech Republic, 2017: pp. 219–226. https://doi.org/10.3384/ecp17132219.

[5] F. Jorissen, Toolchain for Optimal Control and Design of Energy Systems in Buildings, PhD thesis, KU Leuven, 2018.

[6] F. Jorissen, G. Reynders, R. Baetens, D. Picard, D. Saelens, L. Helsen, Implementation and Verification of the IDEAS Building Energy Simulation Library, Journal of Building Performance Simulation. 11 (2018) 669–688. https://doi.org/10.1080/19401493.2018.1428361.

[7] R. Mahmoud, E. Himpe, J. Laverge, D2.2 A set of parametric geometries for the (sub)typologies studied, in: HybridGEOTABS Project (H2020-Project MPC-.GT), Ghent University, Ghent, Belgium, 2020. (confidential).

[8] R. Mahmoud, M. Sharifi, E. Himpe, M. Delghust, J. Laverge, Estimation of load duration curves from general building data in the building stock using dynamic BES-models, E3S Web of Conferences. 111 (2019). http://dx.doi.org/10.1051/e3sconf/201911101078.

[9] H. Cano Esteban, F. Cordero Tosal, S. Dag, Q. Wang, J. Hoogmartens, F. Jorissen, E. Himpe, D6.2 Development and optimisation of individual modules for hybridGEOTABS solutions, in: HybridGEOTABS Project (H2020-Project MPC-.GT), Geoter, Madrid, Spain, 2020. http://www.hybridgeotabs.eu/publications/deliverables.

[10] O.B. Kazançi, D. Khovalyg, B.W. Olesen, Q. Wang, S. Dag, A. Caminade, J. Hoogmartens, J. Cigler, G. Parnis, W. Boydens, H. Cano Esteban, F. Cordero Tosal, J. Borrajo Bastero, E. Himpe, J. Laverge, D6.1 hybridGEOTABS system concept: document defining the system concept, individual modules and interfaces, Danish Technical University, Kopenhagen, Denmark, 2020. http://www.hybridgeotabs.eu/publications/deliverables.

[11] M. Sharifi, R. Mahmoud, E. Himpe, J. Laverge, Integrated Sizing Methodology for a hybridGEOTABS Building, ASHRAE Transactions. 125 (2019) 222–230.

[12] M. Sharifi, E. Himpe, J. Laverge, D2.1 An automated baseload search algorithm for TABS sizing, in: HybridGEOTABS Project (H2020-Project MPC-.GT), Ghent University, Ghent, Belgium, 2019. (confidential).